Comparative Anatomy of α_2 and β Adrenoceptors in the Adult and Developing Brain of the Marine Teleost the Red Porgy (*Pagrus pagrus*, Sparidae): [³H]Clonidine and [³H]Dihydroalprenolol Quantitative Autoradiography and Receptor Subtypes Immunohistochemistry

BASILEIOS ZIKOPOULOS AND CATHERINE R. DERMON*
Laboratory of Neurobiology and Physiology, Department of Biology, University of Crete,
Heraklion 71409, Crete, Greece

ABSTRACT

The present study aimed to determine the anatomic distribution and developmental profile of α_2 and β adrenoceptors (AR) in marine teleost brain. Alpha 2 and β adrenoceptors were studied at different developmental stages by using [³H]clonidine and [³H]dihydroalprenolol, respectively, by means of in vitro quantitative autoradiography. Furthermore, immunohistochemical localization of the receptor subtypes was performed to determine their cellular distribution. Saturation studies determined a high-affinity component of [³H]clonidine and [³H]dihydroalprenolol binding sites. High levels of both receptors were found in preglomerular complex, ventral hypothalamus, and lateral torus. Dorsal hypothalamus and isthmus included high levels of α_2 AR, whereas pretectum and molecular and proliferative zone of cerebellum were specifically characterized by high densities of β AR. From the first year of life, adult levels of both AR were found in most medial telencephalic, hypothalamic, and posterior tegmental areas. Decreases in both receptors densities with age were prominent in ventral and posterior telencephalic, pretectal, ventral thalamic, hypothalamic, and tegmental brain regions. Immunohistochemical data were well correlated with autoradiography and demonstrated the presence of α_{2A}, α_{2C}, β_1, and β_2 AR subtype-like immunoreactivity. Both the neuronal (perikaryal or dendritic) and the glial localization of receptors was revealed. The localization and age-dependent alterations in α_2 and β AR were parallel to plasticity mechanisms, such as cell proliferation in periventricular thalamus, hypothalamus, and cerebellum. In addition, the biochemical characteristics, distribution pattern, and neuronal or glial specificity of the receptors in teleost brain support a similar profile of noradrenergic transmission in vertebrate brain evolution. J. Comp. Neurol. 489:217–240, 2005. © 2005 Wiley-Liss, Inc.

Indexing terms: noradrenergic; cellular localization; saturation kinetics; receptor binding; glia; cell proliferation

Adrenergic receptors interact with noradrenaline, mediating a wide range of physiological actions of noradrenergic neurons originating from locus coeruleus (Smeets and Gonzalez, 2000; Berridge and Waterhouse, 2003). Five main subtypes (α_1, α_2, β_1, β_2, β_3), which are further subdivided into more subgroups, have been identified (Granneman et al., 1991; Bylund, 1992; Nicholas et al., 1993a,b, 1996; Bylund et al., 1994; Civantos-Calzada and Aleixandre-de-Artiñano, 2001). Differential expression of these subtypes in distinct brain regions emphasizes their involvement in a series of events, ranging from stress responses (Flügge et al., 2003), learning (Stamatakis et al., 1998), memory (Ohno et al., 1996), and visual processes (Fernandez-Lopez et al., 1997; Revilla et al., 1998)

to reproductive behavior (Johnson et al., 1988; Ball et al., 1989; Goodman et al., 1996; Riters et al., 2002) and developmental mechanisms (McDonald et al., 1982; Dermon and Kouvelas, 1988; Winzer-Serhan et al., 1997a,b; Winzer-Serhan and Leslie, 1999). Moreover, the noradrenergic system has also been implicated in the neuropathologic state of several diseases, such as schizophrenia and depression (Potter and Manji, 1994; Charney, 1998; Harro and Oreland, 2001).

Although mammalian and avian cerebral adrenoceptors (AR) have been adequately characterized and localized (Palacios and Kuhar, 1980; Unnerstall et al., 1984; Dermon and Kouvelas, 1988), little is known about the teleostean brain AR. Adrenergic receptors of both the α_2 and the β type have been identified in the peripheral nervous system and skin of several teleosts (Holmgren and Nilsson, 1982; Svensson et al., 1993; Katayama et al., 1999). These studies report some differences in the potencies of certain compounds but also point out similarities between vertebrate AR. The AR belong to a conserved gene cluster, and molecular phylogenetic analysis is consistent with the hypothesis that the initial events in generating different adrenergic receptor subtypes were local duplications giving rise to ancestors of the α_1, α_2, and β AR genes. This is suggested for the α_2 AR, and chromosomal mapping in zebrafish determined all three mammalian α_2 AR genes (80–87% identical sequences for transmembrane domains), as well as a fourth duplicated subtype (Ruuskanen et al., 2004). A cross-hybridization study, using different adrenergic receptor probes, identified sequences homologous to human α_{2A} AR in goldfish, frog, turtle, and chicken (Palacios et al., 1989). All residues important for α_2 AR ligand binding are conserved across species and subtypes, and even the more divergent regions of the fish receptors show clear molecular fingerprints typical of a given subtype (Ruuskanen et al., 2004). In addition, Ruuskanen et al. suggested that the events in the generation of diverse α_2 AR (A, B, C) subtypes took place before the divergence of ray-finned fish and tetrapods.

Data on adult and developing cerebral AR type localization are important to correlate with the observed noradrenergic innervation in fish brain (Ekström et al., 1986; Meek et al., 1993; Ma, 1994a,b) and will significantly add to our knowledge on the role of the noradrenergic system in vertebrate classes and the possible adaptive deviations. In this regard, mammalian and avian adrenergic receptor development is well documented, with reported regional receptor density and distribution changes with age (McDonald et al., 1982; Johnson et al., 1984; Jones et al., 1985; Piantanelli et al., 1985; Dermon and Kouvelas, 1988; Erdtsieck-Ernste et al., 1991; Flügge et al., 1993; Winzer-Serhan et al., 1997a,b; Happe et al., 1999; Winzer-Serhan and Leslie, 1999). For this, we aimed to study two major cerebral AR types (α_2 and β) during selected developmental stages of a cultured marine species, the red porgy, *Pagrus pagrus*, a widely distributed Mediterranean and Atlantic sparid of high commercial importance for aquaculture (Kentouri et al., 1994). Although it is known that the marked variability in the brain organization is related only to the phylogenetic history of teleosts but also to functional specializations (Kotrschal et al., 1998), the red porgy, representing modern percomorphs (an order comprising numerous species), provides an important sexual plasticity model (Zikopoulos et al., 2000). Studies on wild populations revealed an unbalanced sex ratio in favor

of females (Manooch and Hassler, 1978; Vassilopoulou and Papaconstantinou, 1992; Harris and McGovern, 1997), and further studies on gonad development of cultured populations have verified that this species is a protogynous sequential hermaphrodite sparid teleost (Kokokiris et al., 1999). Although the exact mechanism of sex reversal is not yet understood, central neurohormonal influences on natural sex change (Eckstein et al., 1979; Holland et al., 1998) and sex-specific cell genesis in the hypothalamus (Zikopoulos et al., 2001) have been implicated.

To determine the levels of α_2 and β receptor proteins, their properties, and their regional and cellular specificity, we adjusted and utilized in vitro receptor autoradiographic and immunohistochemical methods, which combine quantitative mapping of receptor binding sites at different stages with high anatomical and cellular resolution. As a result, the present study provides, for the first time, data on the quantitative distribution, biochemical properties, and detailed cytoarchitectonic localization of α_2 and β AR in the brain of young, juvenile, and adult marine teleost fish.

MATERIALS AND METHODS
Animal and tissue preparation

All fishes used were born and reared at the Institute of Marine Biology of Crete, and animal experimentation was performed according to the national laws on Protection and Welfare of Animals and the European Communities Council directive (86/609/EEC) for the care and use of laboratory animals. Brains of 24 female *Pagrus pagrus* teleosts, aged 6 months to 6 years, separated into four distinct age groups (0+, 2+, 3+, 5+ years) were used.

The rationale for the use of female animals was based on the protogynous hermaphroditic nature of this species. This resulted in an unbalanced sex ratio in favor of females in wild and cultured populations, so individuals can be solely female at younger ages (0+, 2+). Furthermore, studies on the noradrenergic receptors should take into account sexual dimorphism and group or treat different sexes separately, because it has been shown that adrenergic receptors control sexually dimorphic reproductive processes, and their densities correlate well with steroid hormonal levels in birds (Ball et al., 1989; Riters et al., 2002) and mammals (Johnson et al., 1984; Flügge et al., 1992; Etgen and Karkanias, 1994; Shishkina et al., 2001; Dygalo et al., 2002). Such sexual dimorphism is also present in teleosts (our unpublished observations) but is beyond the scope of this study and will be presented in detail in a subsequent publication.

Animals were divided into four distinct age groups, additionally defined by their hormonal levels, which in turn determined their maturation stage (Kokokiris et al., 1999). Specifically, the animals aged 0+ (6–12 months old) were defined as immature, whereas those aged 5+ were characterized as mature (reproductively active). Studies on various sparids indicate that most major developmental events regarding feeding, swimming, and schooling behaviors are completed shortly after hatching, during the first few months of life (Divanach et al., 1993), and they correlate well with the reported postembryonic morphogenesis and regional volumetric growth of the brain (Toyoda and Uematsu, 1994). All fishes used in this

study were at least 6 months old and were more or less fully developed, and the major factor governing the rest of their developmental progress was alterations in hormonal levels defining growth, sexual maturation, and reproductive behavior.

For autoradiographic studies, protein extraction, and Western blotting, animals were killed by decapitation; their brains were rapidly removed, frozen at $-40°C$ in dry-ice cooled isopentane, and kept at $-80°C$ until further use. Brain tissue from adult Wistar rats was also used in the Western blotting analysis for comparison reasons. Coronal and sagittal sections, 10 μm thick, were obtained with a Leica CM 1500 cryostat, mounted on chrome alum/ gelatin-coated slides, and left to dry before autoradiographic binding experiments.

For immunohistochemistry, fish were deeply anesthetized with ethylene glycol monophenyl ether (0.4 ml/liter) and transcardially perfused with saline, followed by a fixative solution [4% PFA in 0.01 M phosphate-buffered saline (PBS), pH 7.4]. The brains were removed, refrigerated overnight in the same fixative with 20% sucrose for postfixation and cryoprotection, and frozen in isopentane at $-40°C$. Free-floating transverse cryosections 50 μm thick were cut and collected in a phosphate buffer solution (0.1 M PB, pH 7.4). Adjacent sections were used in all receptors binding and single- and double-immuno-histochemical protocols to facilitate comparisons.

In vitro receptor autoradiography: saturation and localization studies

The α_2 AR agonist [3H]clonidine (24 Ci/mmol; Amersham Biosciences Europe GmbH, Freiburg, Germany) and the β AR antagonist [3H]dihydroalprenolol (DHA; 56 Ci/ mmol; Amersham Biosciences Europe GmbH) were used to determine the ligand-specific binding sites by means of in vitro autoradiographic techniques. For the saturation studies, the concentration of [3H]clonidine ranged from 0.8 to 8 nM and that of [3H]DHA from 0.4 to 10 nM. For the quantitative localization studies, the tritiated ligands were used at a concentration of 4 nM ([3H]clonidine) or 1 nM ([3H]DHA) for α_2 and β AR, respectively. Nonspecific binding was determined in the presence of 10 μM clonidine (Tocris Cookson, Lancford, Bristol, United Kingdom) and 10 μM propranolol (Sigma, Steinheim, Germany) for α_2 and β AR, respectively. To exclude possible nonspecific α_1 AR binding, the α_1 and α antagonists prazosin (10 μM; Sigma) and phentolamine (100 μM; Sigma) were also used. To determine the presence of β_1 and β_2 AR subtypes in a number of different brain nuclei, the highly selective antagonists Betaxolol hydrochloride (BHCl; 10 μM; Tocris Cookson) for β_1 or ICI 118551 (10 μM; Tocris Cookson) for β_2 were coincubated with radiolabeled ligand.

Adjacent tissue sections were prewashed in 50 mM Tris-HCl buffer, pH 7.7, at 4°C for 30 minutes before incubation at room temperature with [3H]clonidine (60 minutes) or [3H]DHA (50 minutes) at the afore-mentioned concentrations. Free radioligand was removed by washes in ice-cold Tris buffer for 5 and 10 minutes for [3H]clonidine and 2×10 minutes for [3H]DHA, and then sections were dried in a cold air stream. Slides, along with appropriate radioactive standards ([3H]-Microscales; Amersham Biosciences Europe GmbH), were exposed at 4°C for 8–12 months to tritium-sensitive film (Hyperfilm; Amersham

Biosciences Europe GmbH), developed in Kodak D-19, fixed with Agfa Acidofix, and cleared in running water.

Quantitative image analysis

Quantitative analysis of the autoradiograms was performed by using a computerized image-analysis system comprising a black-and-white Sony XC-77CE CCD camera connected to a G4 Macintosh via a Scion LG-3 frame grabber (Scion Corporation, Frederick, MD). NIH Image software (NIH, Bethesda, MD; v.1.61) was used for densitometry of various brain nuclei and subsequent expression of specific binding as femtomoles receptor per milligram tissue. Values for the equilibrium dissociation constant (K_d) and the maximal binding sites (B_{max}) for [3H]clonidine and [3H]DHA were determined by using RADLIG-EBDA-LIGAND (Biosoft), an iterative fitting program based on a multisite binding model, expressed by the Scatchard-Rosenthal equation: $B/F = (B/K_d) + (B_{max}/K_d)$, where B = density of bound receptors, B_{max} = total receptor density, and F = free ligand concentration.

Data were statistically analyzed by using one-way analysis of variance (ANOVA; SPSS v. 8; dependent factor: receptor density, independent factor: age; $P < 0.05$). Post hoc analysis with the LSD test was performed to identify possible differences among the age groups.

Immunohistochemical localization of receptors

Sections were thoroughly washed in PBS (0.01 M, pH 7.4), followed by 1.5% normal horse serum, 5% bovine serum albumin (BSA), and 0.3% Triton X-100 in 0.01 M PBS blocking solution for 60 minutes at room temperature (RT). For single labeling, sections were washed for 10 minutes at RT with 3% H_2O_2 in PBS to suppress endogenous peroxidase activity and were rinsed in buffer prior to blocking. They were then incubated for 48 hours at 10°C with one of the following polyclonal antibodies (Santa Cruz Biotechnology, Santa Cruz, CA; diluted 1:50 in 0.3% Triton X-100 in 0.01 M PBS): goat anti-α_{2A} AR, goat anti-α_{2C} AR, rabbit anti-β_1 AR, rabbit anti-β_2 AR. The sections were rinsed in PBS and incubated with a biotynilated anti-goat or anti-rabbit antibody solution (Vector, Peterborough, United Kingdom; diluted 1:200 in 0.01 M PBS) for 2 hours at RT, followed by an avidin-biotin-peroxidase solution (Vector ABC Elite kit; diluted 1/100A and 1/100B in 0.1% Triton X-100 in 0.01 M PBS) for 1 hour in the dark at RT. Immunoreactive cells were visualized by the peroxidase-catalyzed polymerization of 0.05% 3,3'-diaminobenzidine tetrahydrochloride (DAB; Vector) in 0.01% H_2O_2 buffer solution (pH 7.5). The sections were washed repeatedly in cold buffer, mounted on chrome alum/gelatin-coated slides, and left to dry. To facilitate the identification of brain areas and to enhance contrast, methyl green was used as a counterstain (Sigma; 1% methyl green in ddH_2O). Slides were dehydrated and coverslipped with entellan.

For double-labeling experiments, sections were incubated in a cocktail of primary antibodies for α_{2A} or α_{2C} and β_1 or β_2 AR (each diluted 1:50 in 0.3% Triton X-100 in 0.01 M PBS) as well as each AR antibody with antiglial fibrillary acidic protein (GFAP; Boehringer Mannheim GmbH-Germany; diluted 1:100 in 0.3% Triton X-100 in 0.01 M PBS) for 48 hours at 10°C, to examine close interactions of those receptor systems as well as possible colocalization with astroglia. Secondary antibodies, anti-goat Alexa

Fluor 568 and anti-rabbit Alexa Fluor 488 (Molecular Probes, Leiden, The Netherlands; diluted 1:500 in 0.3% Triton X-100 in 0.01 M PBS), were also added simultaneously for 2 hours at RT in the dark. Finally, sections were thoroughly rinsed, mounted on chrome alum/gelatin-coated slides, and left to dry before coverslipping with Prolong Antifade (Molecular Probes). In addition, the cytoarchitecture of different brain areas was determined in sections stained with cresyl violet (Sigma; 0.5% cresyl violet in ddH$_2$O), and the nomenclature used was based on that of Northcutt and Davis (Braford and Northcutt, 1983; Nieuwenhuys and Pouwels, 1983; Northcutt and Davis, 1983), supplemented by Maler et al. (1991) and Wullimann et al. (1996).

Specificity of antibodies

To test the specificity of the immunoreactivity of antibodies used in the teleost tissue, proper controls were

performed. Control experiments, with sections adjacent to those used in the experiments described above, included 1) incubation omitting the primary antibodies, 2) application of secondary antisera mismatched for species, and 3) application of preincubated primary antibody with excess of the proper specific peptides (Santa Cruz Biotechnology; sc 569 for β_2 AR, sc 567 for β_1AR, sc 1478 for α_{2A} AR, or sc 1480 for α_{2C} AR) used to raise the antibodies. All control experiments resulted in no immunocytochemical labeling. In addition, Western immunoblot experiments were conducted to compare the migration of the immunoreacting proteins in mammalian and teleostean brains.

Western immunoblot procedure

Fish and rat brain tissue was homogenized with a Teflon-glass homogenizer in 0.01 M PBS, pH 7.4, containing 1% Triton X-100 (Sigma), 0.5% sodium deoxycholate (Sigma), and 0.05% sodium dodecyl sulfate (SDS; Sigma). Iodoacetamide (1 mM; Sigma), 0.4 mM phenylmethylsulfonyl fluoride (PMSF; Sigma), and 1 µM pepstatin A (Sigma) were used as protease inhibitors. The tissue homogenates were incubated in ice for 1 hour and further homogenized by passing through a 22-gauge needle. Remaining cell debris was removed by briefly centrifuging at 8,000 rpm for 20 minutes at 4°C. The supernatant was used for protein concentration determination with the Lowry assay and subsequently diluted with loading buffer (2 ml 0.5 M Tris-HCl, 1.6 ml glycerol, 3.0 ml 10% SDS, 0.8 M mercaptoethanol, 0.4 ml 0.05% bromophenol blue) and boiled for 5 minutes at 95°C. Twenty micrograms of protein were separated electrophoretically on a 10% SDS-polyacrylamide gel.

The separated proteins were transferred to a methanol-activated Parablot-PVDF membrane (Macherei-Nagel) at 400 mA for 2 hours at 4°C that was subsequently stained briefly with Poinceau red to verify protein transfer. After blocking with 5% dried skimmed milk, 1% normal horse serum (NHS) in PBST (0.05% Tween in 0.01 M PBS) for 60 minutes, the AR were detected by incubating the PVDF filter at 10°C for 48 hours with one of the following polyclonal antibodies

TABLE 1. Kinetic Analysis of [³H]Clonidine Binding in Teleost Brain[1]

	K_d (nM)	B_{max} (fmoles/mg)
Dorsal telencephalon		
Adult	1.89 ± 0.5	19 ± 2[2]
Young	1.84 ± 0.9	33 ± 6
Ventral telencephalon		
Adult	1.66 ± 0.1	22 ± 4[2]
Young	1.50 ± 0.2	15 ± 5
Dorsal thalamus		
Adult	1.10 ± 0.1	20 ± 1
Young	1.26 ± 0.6	22 ± 3
Ventral thalamus		
Adult	1.30 ± 1.0	10 ± 2[2]
Young	1.76 ± 0.6	24 ± 3
Ventral hypothalamus		
Adult	1.89 ± 0.7	20 ± 3[2]
Young	1.60 ± 0.8	24 ± 5
Locus coeruleus		
Adult	1.49 ± 0.2	30 ± 1[2]
Young	1.80 ± 0.9	47 ± 9

[1]Values are shown as mean ± SEM. In all brain areas presented here, statistically significant differences were detected in the localization experiments (for details see text).
[2]Up- or down-regulation of receptor density detected throughout the brain at various ages is the result of differences in the number of binding sites rather than in receptor affinity, with the exception of dorsal thalamus, where no apparent changes in K_d or B_{max} are detected.
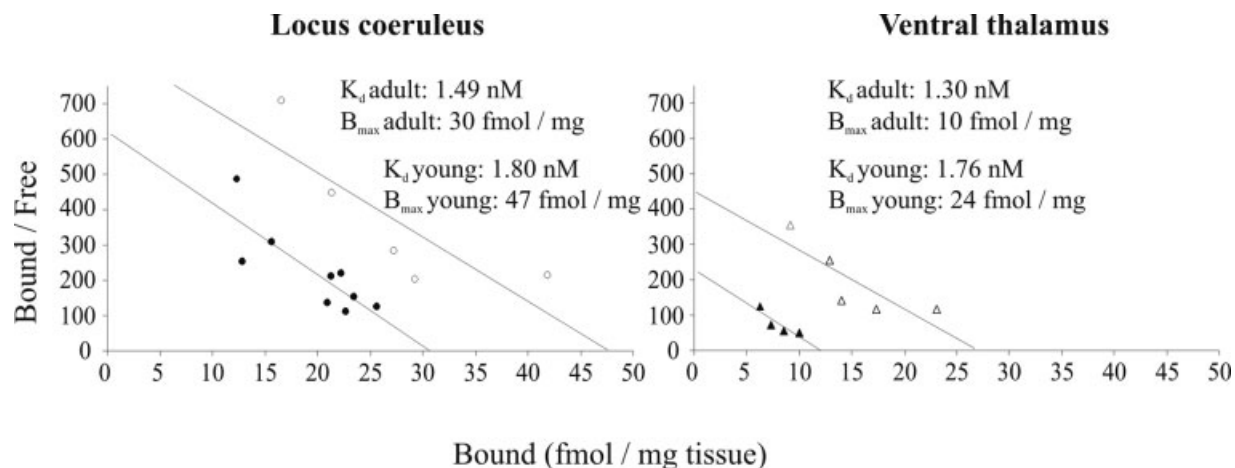

Fig. 1. Kinetic properties of [³H]clonidine binding as determined by autoradiographic saturation analysis in various teleost brain areas. Scatchard plots of some regions are presented (for more details see text and Table 1). Solid symbols depict values from adult animals, whereas open symbols correspond to values from young animals.

(Santa Cruz Biotechnology; diluted 1:100 in PBST with 2% dried skimmed milk): goat anti-α_{2A} AR, goat anti-α_{2C} AR, rabbit anti-β_1 AR, rabbit anti-β_2 AR. After three washes in PBST for 10 minutes each, the membranes were incubated for 2 hours at RT with secondary anti-rabbit or anti-goat IgG antibodies (Vector ABC Elite kit) diluted 1/2,000 in PBST, followed by an

avidin-biotin-peroxidase solution (Vector ABC Elite kit; diluted 1/1,000 A and 1/1,000 B in PBST) for 1 hour at RT. Bands were visualized by the peroxidase-catalyzed polymerization of 0.05% 3,3'-diaminobenzidine tetrahydrochloride (DAB; Vector) in 0.01% H_2O_2 buffer solution (pH 7.5). Rat brain homogenates were used as positive controls, whereas omission of primary antisera provided the necessary negative controls.

Preparation of figures

Selected images from film autoradiograms were digitized with the black-and-white image-analysis system mentioned above. High-resolution photomicrographs were taken with a color 3CCD Sony DXC-950P camera on a Nikon Eclipse E800 microscope connected to a PC via a Scion CG-7 frame grabber (Scion Corp.). Figures were prepared with Adobe Photoshop (Adobe Systems Inc., San Jose, CA), and overall brightness and contrast were adjusted without retouching.

TABLE 2. Kinetic Analysis of [³H]Dihydroalprenolol Binding in Teleost Brain and Quantitative (% of Total β AR Binding) β_1 and β_2 AR Subtype Distribution[1]

	K_d (nM)	B_{max} (fmoles/mg)	β_1 (%)	β_2 (%)
Central part of the dorsal telencephalon				
Adult	1.30 ± 0.1	27 ± 4	21	27
Young	1.27 ± 0.3	23 ± 2	23	29
Dorsal part of the dorsal telencephalon				
Adult	0.75 ± 0.2	23 ± 2	15	40
Young	0.42 ± 0.1	25 ± 1	22	42
Lateral part of the dorsal telencephalon				
Adult	1.10 ± 0.6	35 ± 7	40	70
Young	1.10 ± 0.5	30 ± 6	35	60
Medial part of the ventral telencephalon				
Adult	1.15 ± 1.0	20 ± 6[2]	13	19
Young	1.26 ± 0.5	31 ± 4	38	19
Dorsal thalamus				
Adult	1.24 ± 0.1	20 ± 2[2]	43	80
Young	1.21 ± 0.8	34 ± 9	84	43
Ventral hypothalamus				
Adult	0.78 ± 0.1	18 ± 1[2]	34	54
Young	0.94 ± 0.1	27 ± 1	29	41
Locus coeruleus				
Adult	0.95 ± 0.3	22 ± 3[2]	33	63
Young	0.84 ± 0.2	43 ± 4	23	31
Molecular cerebellar layer				
Adult	1.67 ± 0.3	38 ± 2	39	79
Young	1.58 ± 0.3	45 ± 7	27	74

[1]Values for K_d and B_{max} are shown as mean ± SEM. In most brain areas presented here, statistically significant differences were detected in the localization experiments (for details see text). Relative proportions (%) of β_1 and β_2 AR reveal predominance of β_2 AR and decline in β_1 AR levels with age in most areas that show age-related differences.
[2]As in the case of α_2 AR, down-regulation of receptor density detected throughout the brain at various ages is the result of differences in the number of binding sites rather than in receptor affinity.

RESULTS
Saturation analysis of [³H]clonidine and [³H]DHA binding sites in young and adult teleost brain

Scatchard analysis of [³H]clonidine binding showed saturable high-affinity binding in all the brain areas, with K_d values ranging between 1.1 and 1.9 nM (Table 1, Fig. 1). Dorsal thalamic areas exhibited the highest affinity (K_d 1.1–1.8 nM) and moderate densities (B_{max} 20 fmoles/mg tissue) of α_2 AR. Radioligand binding in telencephalic, diencephalic, and tegmental areas revealed curves with slightly decreased affinity (K_d 1.5–1.9 nM) and maximal densities up to 47 fmoles/mg tissue. The level of nonspecific binding ranged between 5% and 10% in all cases in which cold drugs (clonidine, phentolamine, or prazosin) were used.

Scatchard plots of [³H]DHA binding showed a saturable high-affinity component, with K_d values ranging between
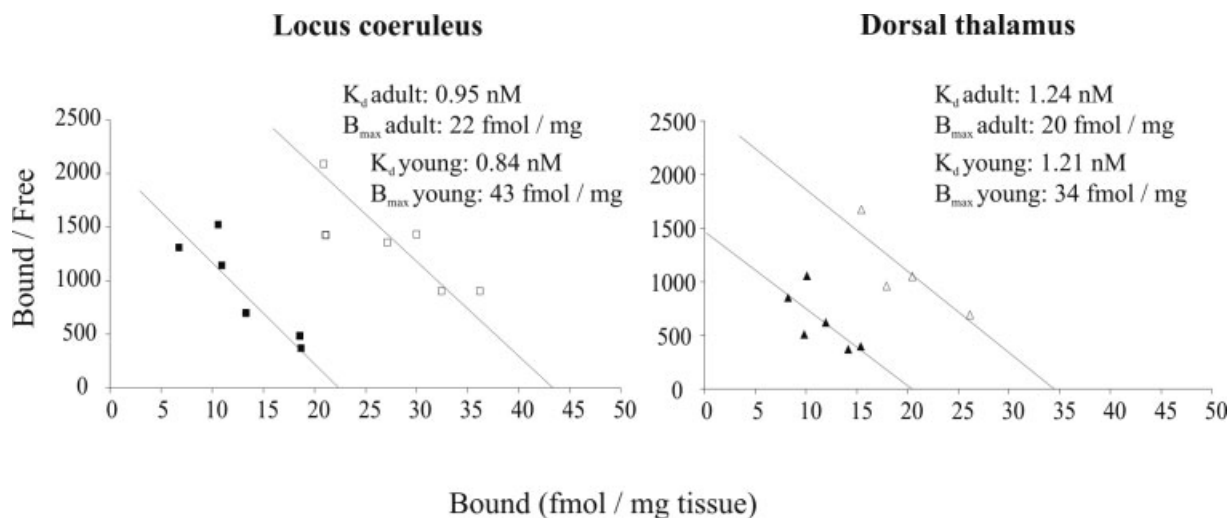

Fig. 2. Kinetic properties of [³H]dihydroalprenolol binding as determined by autoradiographic saturation analysis in various teleost brain areas. Scatchard plots of some regions are presented (for more details see text and Table 2). Solid symbols depict values from adult animals, whereas open symbols correspond to values from young animals.

TABLE 3. Quantitative Distribution of α_2 AR (fmoles/mg Tissue ± SEM) in Young and Adult Teleosts (Red Porgy, *Pagrus pagrus*)[1]

Area	Age (years)			
	0+	2+	3+	5+
Dorsal telencephalon				
Medial zone 1 of the dorsal telencephalic area (Dm1)	15.7 ± 2.7	11.3 ± 2.1	11.4 ± 0.4	14.2 ± 3.3
Medial zone 2 of the dorsal telencephalic area (Dm2)	18.1 ± 4.2	11.6 ± 1.9[2]	12.0 ± 1.1[2]	14.0 ± 1.8[2]
Medial zone 3 of the dorsal telencephalic area (Dm3)	15.8 ± 2.9	13.8 ± 3.0	12.2 ± 0.6	16.7 ± 2.3
Medial zone 4 of the dorsal telencephalic area (Dm4)	26.6 ± 7.1	13.8 ± 2.6[2]	10.6 ± 0.1[2]	16.9 ± 3.3[2]
Central zone of the dorsal telencephalic area (Dc)	13.4 ± 1.1	13.6 ± 2.7	12.7 ± 2.0	16.7 ± 2.0
Dorsal zone of the dorsal telencephalic area (Dd)	12.2 ± 1.4	11.5 ± 1.9	12.0 ± 2.1	13.5 ± 2.0
Dorsal part of the lateral zone of the dorsal telencephalic area (Dld)	14.1 ± 2.3	12.7 ± 2.7	11.3 ± 0.1	16.3 ± 2.4
Ventral part of the lateral zone of the dorsal telencephalic area (Dlv)	14.0 ± 2.4	13.0 ± 2.2	12.1 ± 1.1	18.1 ± 2.2
Lateral part of the lateral zone of the dorsal telencephalic area (Dll)	14.0 ± 1.5	13.9 ± 2.7	11.5 ± 1.3	14.3 ± 2.4
Posterior part of the lateral zone of the dorsal telencephalic area (Dlp)	13.9 ± 1.3	15.0 ± 2.8	12.0 ± 0.9	12.2 ± 2.7
Posterior zone of the dorsal telencephalic area (Dp)	17.3 ± 2.4	17.1 ± 3.5	14.0 ± 4.0	12.8 ± 2.4
Ventral telencephalon				
Olfactory bulb (OB)	11.4 ± 1.1	7.8 ± 0.2	9.3 ± 2.7	11.0 ± 2.6
Ventral nucleus of the ventral telencephalic area (Vv)	17.7 ± 2.2	14.6 ± 2.4	10.5 ± 0.1	19.0 ± 2.0[4]
Lateral nucleus of the ventral telencephalic area (Vl)	14.8 ± 1.7	18.2 ± 3.4	11.8 ± 3.5	14.0 ± 1.5
Dorsal nucleus of the ventral telencephalic area (Vd)	21.1 ± 3.4	12.8 ± 1.3[2]	11.2 ± 1.3[2]	16.1 ± 2.3
Supracommissural nucleus of the ventral telencephalic area (Vs)	26.0 ± 3.9	14.5 ± 1.8[2]	10.7 ± 1.3[2]	18.3 ± 3.9[2]
Central nucleus of the ventral telencephalic area (Vc)	12.6 ± 1.3	14.2 ± 3.0	12.3 ± 2.3	14.7 ± 1.7
Pretectum				
Superficial pretectal nucleus, parvocellular portion (PSp)	16.1 ± 1.1	14.5 ± 1.6	12.4 ± 3.4	9.8 ± 1.6[2]
Superficial pretectal nucleus, magnocellular portion (PSm)	12.4 ± 1.1	11.5 ± 2.8	12.2 ± 3.6	9.3 ± 1.9
Dorsal periventricular pretectal nucleus (PPd)	16.1 ± 1.1	11.5 ± 0.9	8.9 ± 2.5	9.6 ± 1.2[2]
Ventral periventricular pretectal nucleus (PPv)	18.6 ± 0.8	12.1 ± 1.4[2]	8.5 ± 1.9[2]	10.2 ± 1.2[2]
Dorsal thalamus				
Habenulla (Ha)	4.1 ± 0.5	5.2 ± 1.7	5.5 ± 0.9	4.5 ± 1.4
Dorsal posterior thalamic nucleus (DP)	10.7 ± 1.2	11.1 ± 1.5	8.9 ± 1.3	10.0 ± 1.4
Central posterior thalamic nucleus (CP)	16.0 ± 0.6	13.0 ± 1.4	8.1 ± 0.3[2]	10.2 ± 1.2
Ventral thalamus				
Ventromedial nucleus (VM)	21.0 ± 1.3	12.4 ± 2.4[2]	7.2 ± 0.9[2]	10.0 ± 1.1[2]
Ventrolateral nucleus (VL)	21.5 ± 1.2	12.9 ± 2.1[2]	8.7 ± 0.9[2]	9.6 ± 0.8[2]
Periventricular nucleus of the posterior tuberculum (TPp)	25.9 ± 2.6	19.4 ± 2.3[2]	11.0 ± 1.8[2,3]	14.6 ± 1.4[2]
Pre-/glomerular complex				
Medial preglomerular nucleus (PGm)	25.1 ± 3.0	23.1 ± 4.9	18.3 ± 4.2	19.4 ± 1.3
Lateral preglomerular nucleus (PGl)	26.2 ± 3.0	22.2 ± 3.7	16.0 ± 0.5[2]	15.6 ± 1.6[2,3]
Glomerular nucleus (G)	7.6 ± 0.7	5.7 ± 1.0	4.1 ± 0.6	2.6 ± 0.8
Preoptic area				
Medial magnocellular preoptic nucleus (PMm)	14.9 ± 1.3	9.7 ± 1.3	9.4 ± 1.9	10.1 ± 1.7
Posterior parvocellular preoptic nucleus (PPp)	14.5 ± 1.2	10.1 ± 0.9	8.4 ± 1.1	10.5 ± 1.7
Anterior parvocellular preoptic nucleus (PPa)	17.3 ± 1.8	11.7 ± 1.1	10.9 ± 0.8	14.8 ± 2.7
Suprachiasmatic nucleus (SC)	13.6 ± 2.0	10.2 ± 1.3	8.7 ± 1.5	12.7 ± 1.2
Dorsal hypothalamus				
Dorsal hypothalamic area (dHA)	28.7 ± 3.0	20.3 ± 2.7[1]	14.2 ± 2.1[2]	19.1 ± 2.3[2]
Nucleus of the lateral recess (nRL)	25.6 ± 2.8	20.3 ± 2.7	14.2 ± 2.1[2]	18.6 ± 2.3[2]
Paraventricular organ (PVO)	30.9 ± 3.0	22.9 ± 4.1[2]	15.1 ± 3.0[2]	21.1 ± 3.2[2]
Anterior tuberal nucleus (TA)	23.3 ± 1.3	15.7 ± 1.4[2]	11.6 ± 1.9[2]	13.4 ± 1.6[2]
Mammillary corpus (CM)	21.4 ± 2.3	19.9 ± 2.6	11.3 ± 0.7[2,3]	16.2 ± 1.8
Ventral hypothalamus				
Lateral tuberal nucleus (nLT)	17.9 ± 1.7	13.2 ± 1.8	9.6 ± 0.9[2]	13.3 ± 2.4
Nucleus of the lateral hypothalamus (LH)	24.3 ± 1.9	16.3 ± 1.1[2]	11.5 ± 2.8[2]	15.5 ± 2.6[2]
Nucleus of the periventricular ventral hypothalamus (Hv)	32.5 ± 2.7	23.9 ± 2.6[2]	16.4 ± 1.1[2]	27.3 ± 3.2[4]
Nucleus of the periventricular caudal hypothalamus (Hc)	26.1 ± 3.2	28.9 ± 6.0	13.2 ± 1.1[2,3]	22.0 ± 2.3[3,4]
Lateral torus-inferior lobe				
Diffuse nucleus of the lateral torus (NDTL)	23.3 ± 1.3	25.0 ± 4.0	15.9 ± 0.6	18.1 ± 2.0[3]
Anterior nucleus of the central part of the inferior lobe (NCILa)	23.7 ± 1.2	20.3 ± 4.1	17.7 ± 2.7	20.8 ± 2.1
Posterior nucleus of the central part of the inferior lobe (NCILp)	23.3 ± 4.3	23.5 ± 4.4	20.9 ± 6.0	20.5 ± 3.3
Central nucleus of the inferior lobe (CE)	22.3 ± 1.9	18.9 ± 3.6	16.3 ± 3.5	18.0 ± 3.0
Diffuse nucleus of the inferior lobe (DIF)	23.1 ± 2.3	16.9 ± 2.5[2]	11.6 ± 0.6[2]	16.1 ± 1.8[2]
Optic tectum				
Stratum opticum (SO)	7.2 ± 0.6	4.0 ± 0.8	2.6 ± 0.9	1.8 ± 0.7
Stratum griseum centrale (SGC)	9.9 ± 1.1	9.6 ± 2.8	7.7 ± 0.3	7.8 ± 2.6
Stratum fibrosum et griseum superficiale (SGFS)	15.0 ± 0.9	9.8 ± 1.8	5.0 ± 1.8[2]	8.3 ± 1.8[2]
Stratum griseum periventriculare (SGP)	18.8 ± 1.9	14.7 ± 3.6	10.0 ± 0.4[2]	13.7 ± 2.0
Stratum album centrale (SAC)	9.2 ± 1.5	3.8 ± 1.2	0.1 ± 0.8[2]	3.0 ± 1.7[2]
Semicircular torus				
Semicircular torus, layer 1 (TS1)	8.3 ± 3.2	4.8 ± 1.7	3.8 ± 0.2	3.8 ± 1.3
Semicircular torus, layer 2 (TS2)	11.5 ± 3.3	7.8 ± 1.4	5.3 ± 0.2	7.1 ± 1.7
Semicircular torus, layer 3 (TS3)	7.9 ± 1.4	6.8 ± 0.6	3.7 ± 1.4	4.4 ± 1.4
Semicircular torus, layer 4 (TS4)	8.0 ± 2.0	8.3 ± 1.7	5.9 ± 0.3	4.1 ± 1.4
Isthmic area-midbrain tegmentum				
Locus coeruleus (LoC)	44.6 ± 8.4	34.0 ± 6.6[2]	20.1 ± 5.4[2,3]	24.9 ± 3.0[2,3]
Isthmic nucleus (is)	23.7 ± 4.8	20.7 ± 6.0	14.0 ± 2.6[2]	17.3 ± 1.3[2]
Cortical nucleus (NC)	18.0 ± 2.4	14.0 ± 0.7	10.7 ± 1.3	10.7 ± 2.0[2]
Nucleus of the medial longitudinal fascicle (nuflm)	26.3 ± 0.7	14.6 ± 2.1[2]	7.6 ± 0.9[2]	11.9 ± 1.5[2]
Medial longitudinal fascicle (flm)	7.1 ± 1.1	5.3 ± 1.9	1.3 ± 0.5	3.5 ± 2.0
Oculomotor nucleus (NIII)	20.7 ± 1.4	18.6 ± 2.3	8.6 ± 1.2[2,3]	13.6 ± 1.6[2]
Central grey (GC)	13.6 ± 2.5	8.4 ± 0.4	7.2 ± 1.7	9.4 ± 1.9
Dorsal raphe (Rd)	12.0 ± 0.7	11.1 ± 0.9	8.0 ± 3.2	7.2 ± 1.5
Medial raphe (Rm)	11.8 ± 0.9	11.7 ± 1.3	7.9 ± 2.9	7.4 ± 1.5
Interpeduncular nucleus (NIn)	15.3 ± 0.9	11.4 ± 1.0	9.3 ± 1.1	7.4 ± 1.6[2]
Motor nucleus of the trigeminal nerve (NVm)	19.9 ± 1.4	13.5 ± 0.8[2]	8.6 ± 0.7[2]	11.0 ± 2.7[2]
Inferior reticular nucleus (ri)	13.7 ± 0.3	10.5 ± 0.3	9.1 ± 0.7	8.2 ± 0.7
Medial reticular nucleus (rm)	11.5 ± 1.5	10.0 ± 0.2	8.9 ± 1.0	8.5 ± 1.0
Superior reticular nucleus (rs)	15.8 ± 0.7	11.7 ± 0.4	10.0 ± 1.2	9.7 ± 0.8[2]
Inferior olive (oli)	13.6 ± 0.7	11.1 ± 0.8	10.0 ± 1.2	9.4 ± 0.8

TABLE 3. (continued)

Area	Age (years)			
	0+	2+	3+	5+
Cerebellum-accessory cerebellar nuclei				
Longitudinal torus (tlo)	5.3 ± 1.2	2.2 ± 0.7	1.5 ± 1.4	1.9 ± 0.7
Nucleus of the lateral valvula (lv)	14.0 ± 1.6	6.8 ± 2.2[2]	4.9 ± 2.4[2]	5.9 ± 2.0[2]
Lateral granular eminence (Egl)	10.2 ± 0.7	5.6 ± 1.6	6.3 ± 0.5	4.6 ± 0.9
Medial granular eminence (Egm)	9.4 ± 1.5	5.4 ± 1.3	3.4 ± 1.1	4.2 ± 0.7
Granular layer of the valvular cerebelli (VCbgr)	9.1 ± 1.8	3.3 ± 1.3	3.0 ± 0.4	3.2 ± 1.0
Molecular layer of the valvular cerebelli (VCbmol)	4.9 ± 0.8	2.6 ± 0.7	1.3 ± 0.9	1.5 ± 0.6
Granular layer of the cerebellar corpus (CCbgr)	11.1 ± 1.4	6.4 ± 1.1	4.8 ± 1.3	4.1 ± 0.7[2]
Molecular layer of the cerebellar corpus (CCbmol)	6.8 ± 1.6	2.6 ± 0.7	1.8 ± 0.3	2.3 ± 0.8
Medial proliferation zone of the cerebellar corpus (CCbPZ)	20.0 ± 0.3	18.6 ± 2.9	11.7 ± 0.6[2]	12.1 ± 2.8[2,3]
Overall	9.3 ± 1.0	5.8 ± 0.8	4.6 ± 0.0	7.2 ± 1.0

[1]Footnotes 2–4 highlight significant differences (one-way ANOVA, dependent factor: receptor density, independent factor: age, $P < 0.05$, LSD post hoc test).
[2]Significant difference with the age 0+.
[3]Significant difference with the age 2+.
[4]Significant difference with the age 3+.

0.4 and 1.7 nM. Some dorsal and caudal forebrain areas and most hypothalamic regions exhibited the relatively highest affinity (K_d 0.42–1.1 nM) and average levels of B_{max} values (18–35 fmoles/mg tissue; Table 2, Fig. 2). Nonspecific binding detected with propranolol was 30–40% of total binding, depending on the area measured. Statistical analysis of the parameters of [^{3}H]clonidine and [^{3}H]DHA binding in various representative brain areas of young and adult animals revealed that the age differences in cerebral receptor binding represented differences in the number of binding sites rather than differences in receptor affinity (Tables 1, 2, Figs. 1, 2).

Quantitative distribution of α_2 and β binding sites in developing and adult teleost brain

The distribution of α_2 AR in the teleost brain determined by [^{3}H]clonidine binding was heterogeneous (Table 3, Fig. 3). The highest levels of expression were found in locus coeruleus (LoC), most hypothalamic and preglomerular nuclei, whereas the lowest levels were detected in cerebellar, habenular, and glomerular areas and tracts. Autoradiographic studies with [^{3}H]DHA revealed a much less heterogeneous β AR distribution (Table 4, Fig. 4). Highest receptor densities were measured in pretectal and preglomerular thalamic nuclei as well as lateral hypothalamic and medial brainstem regions. The vast majority of brain areas exhibited moderate β AR densities, whereas tectal and habenular regions showed low binding.

In most brain areas studied, the distribution pattern of α_2 and β AR did not change with age; however, significant changes in the absolute and relative density of both receptors' binding were found in specific brain areas. Based on the developmental pattern of α_2 AR, brain areas that modify their receptor levels can be grouped into those that showed age-related increases in receptor density (e.g., Vv area) and those that showed transient (Dm2, Hc, Hv) or gradual but permanent (Dm4, Vd, Vs, TPp, NIII, LoC) decreases after the age of 0+. In contrast, β AR binding sites showed only negative correlation with age in areas where age-associated changes are observed (OB, Vv, Vs, PPd, VL, CP, PGm, PGl, G, PMm, NCILp, PVO, Hv, LoC, is, NC, nuflm, NIII, NVm, ri, rm, rs, oli, tlo, CCbPZ). The regional profile in detail of receptor binding with age follows.

Telencephalon. All telencephalic areas included moderate levels of α_2 AR, with the ventral parts exhibiting higher levels. Medial areas of the dorsal and ventral tel-

encephalon (Dm2, Dm4, Vd, Vs) showed a gradual decrease in receptor binding with age (Fig. 3A,B). Ventromedial nuclei (Vv), on the other hand, displayed an increase of α_2 receptor levels at the age of 5+ (Table 3). Both elevations and decreases of receptor densities were also reflected by increased or decreased B_{max} values, respectively, whereas K_d values remained similar (Table 1).

Telencephalic β AR distributed homogeneously at moderate levels (Fig. 4A,B). Striking differences in the amount of β AR were apparent mainly at the medial parts dorsally (Dm3, -4) and ventrally (Vv, Vd, Vs) as well as more centrally (Vc) and at the olfactory bulbs (OB), where a gradual decrease with age was observed (Table 4, Fig. 4), and B_{max} values for these areas in younger, immature animals showed higher levels of binding sites than in older, mature animals (Table 2).

Diencephalon. High density of α_2 AR was found in most periventricular hypothalamic regions (Hv, dHA, nRL, PVO, Hc), lateral nuclei of the inferior lobe and tubercle (NCILa, NCILp, CE, NDTL), and the preglomerular complex (PGl, PGm). With the exception of the habenular and glomerular nucleus, which exhibited very low labeling, all other hypothalamic and thalamic areas displayed moderate levels of receptors. Ventral (VM, VL) and central (CP) thalamic and pretectal nuclei (PSp, PPd, PPv) showed a decrease in receptor density with age, whereas the posterior tuberculum (TPp) and the lateral preglomerular nucleus (PGl) displayed a more gradual decrease from immature (0+) to intermediate (2+, 3+) and mature (5+) animals (Table 3, Fig. 3C,D). The ventral periventricular hypothalamus (Hv, Hc) exhibited transient decreases in receptor levels from immature to 3+ females, followed by significant increases in receptor density at 5+. Most other hypothalamic areas followed a pattern of decrease in receptor density with age, which in most cases started after the age 0+, and the reduction continued and remained significant all the way to maturity (DIF, dHA, nRL, PVO, LH, TA). Some nuclei (nLT, CM) showed adult levels of AR at the age of 3+, whereas in the lateral torus (NDTL) the reduction became apparent after the age of 2+ (Table 3). In agreement with this, saturation studies in those areas show decreased B_{max} values in older-mature animals (Table 1).

In the anterior pretectum (PSm, PSp), preglomerular complex (PGm, PGl), and central-lateral hypothalamic nuclei (NCILa, NCILp, NDTL), high densities of β AR were measured (Table 4, Fig. 4C,D). Receptor binding was moderate, similar to that described for the α_2 type for all other
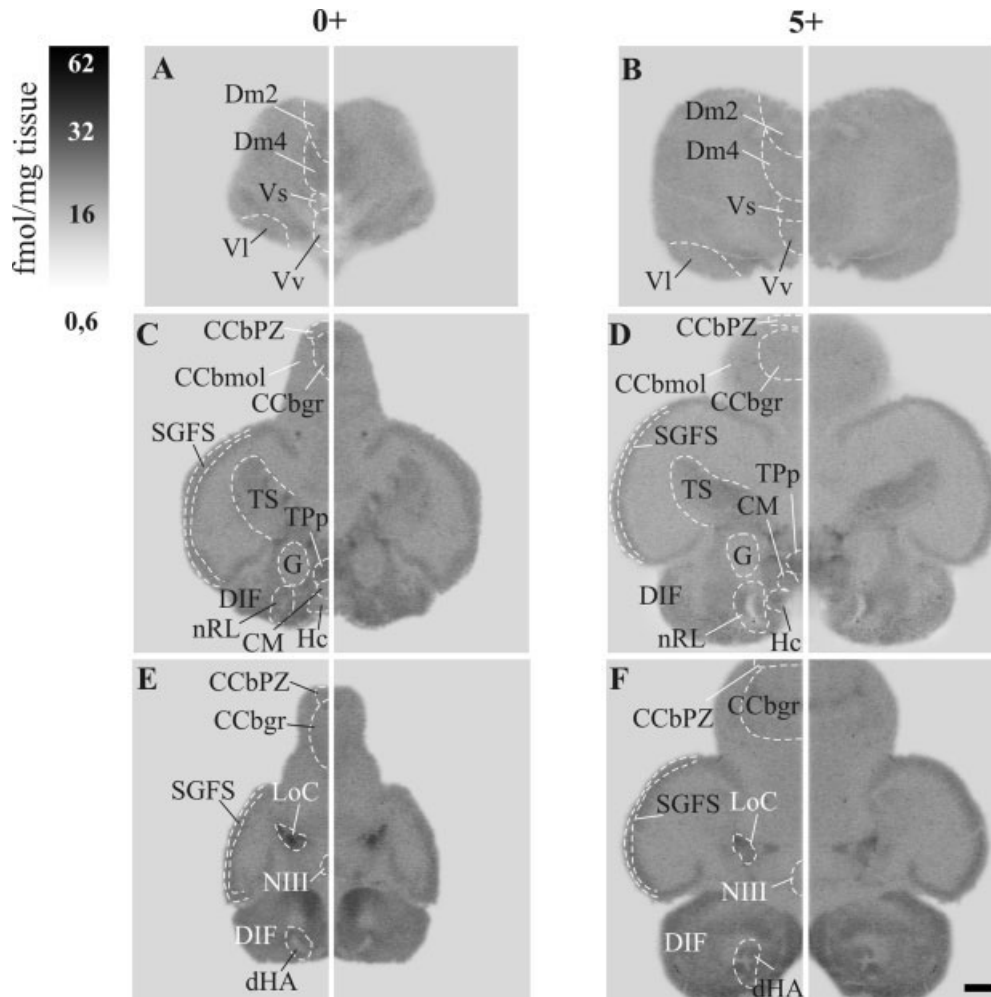
Fig. 3. Autoradiographic images of coronal sections in prosence-phalic (**A,B**), midbrain (**C, D**), and hindbrain (**E,F**) regions of young (0+; A,C,E) and adult (5+; B,D,F) red porgies, showing the regional density of α_2 adrenoceptors and the alterations during development (for details and abbreviations, see text and Table 3). With the exception of ventromedial telencephalic areas (Vv), in most other nuclei the levels of α_2 receptors decrease with age. Scale bar = 2,000 μm in F (applies to A–F).

diencephalic regions except the habenula, which exhibited the lowest labeling. Most thalamic pretectal (PSp, PSm, PPd, PPv), pre- and glomerular (PGl, PGm, G), rostral (VM, VL), and central (DP, CP) nuclei showed decreases in binding with age, in some cases through gradual receptor density reduction (PSp, PSm; Fig. 4C–F). That was also the case for the hypothalamic inferior lobe (NCILa) and lateral torus (NDTL) but not for preoptic (PMm, PPa, SC) and periventricular (Hv, CM, PVO) regions, which exhibited a steeper fall (Table 4). Maximal receptor densities (B_{max}) appeared to be lower in older females, whereas the affinity remained similar (Table 2).

Brainstem and cerebellum. The brainstem and cerebellum exhibited the most heterogeneous α_2 AR binding. The noradrenergic activity center, LoC, displayed by far the highest levels of α_2 AR (Fig. 3E,F). Moderate to high densities were also detected in midbrain tegmentum and isthmic nuclei (nuflm, NIII, is), along with the deepest periventricular tectal layer (SGP). Most other mesencephalic and rhombencephalic regions showed moderate to low receptor levels, and areas rich in fibers (flm, SO, SAC, TS1) were almost devoid of α_2 AR. Low receptor densities were found in cerebellar and accessory cerebellar regions (CCbmol, CCbgr, VCbmol, VCbgr, lv, tlo, Egl, Egm), the only exception being the dorsomedial part of the molecular cerebellar layer (CCbPZ; Table 3, Fig. 3F), which included moderate to high densities. We observed gradual (LoC, NIII) and steeper (nuflm, is, NC, NIn, NVm, rs, SGFS, SGP, SAC, CCbgr, CCbPZ, lv) receptor decreases with age (Fig. 3E,F), a pattern similar to that in the diencephalon. In accordance, related alterations of appropriate B_{max} were determined (Table 1).

Tritiated DHA-specific binding showed high or moderate levels of β AR binding sites. Midbrain tegmentum (NIII), medial hindbrain (Rd, Rm, NIn, NVm), and isthmic (is) nuclei showed high densities of β AR. The lowest labeling was seen in some fibrous tectal layers (SO, SAC). All cerebellar structures and especially the molecular layers (CCbmol, VCbmol, CCbPZ) displayed high densities of binding sites (Table 4, Fig. 4E–H). The number of binding

sites decreased with age in cerebellar (CCbPZ, Egl, Egm) and accessory cerebellar (tlo) nuclei. A similar decrease was observed in LoC, midbrain tegmentum (NIII, nuflm, GC, is, NC, NIn), raphe complex (Rd, Rm), and hindbrain (ri, rm, rs, oli, NVm).

Mammalian AR antibodies recognize teleostean AR-like proteins on Western blots

To verify whether the polyclonal AR subtype-specific antibodies generated against mammalian adrenergic receptor proteins would recognize the homologous proteins from red porgy, protein extracts from rat and red porgy brains were processed by SDS-PAGE and Western blotting. All antibodies detected protein bands migrating at about the same apparent molecular weights (Fig. 5) as the corresponding rat AR proteins, and these are likely to represent the fish homologues of α_{2A}, α_{2C}, β_1, and β_2 AR. Moreover, readsorption of the primary antibodies with excess of the specific peptides, used to raise the specific antibodies, in the presence of the relevant primary and secondary antibodies resulted in lack of labeling in the sections, further supporting the specificity of the antibodies used in the teleost brain.

Anatomical and cellular organization of specific α_2 and β AR subtypes

Four types of neurons exhibiting AR immunoreactivity (-ir) were found: 1) a large (10–15 μm), ovoid, elongated one with thick unipolar or bipolar dendrites; 2) slightly smaller but similar in shape Purkinje cells; 3) a medium-sized (6–10 μm) one, usually with fine varicose fibers; and 4) a small, round, granular type cell. In addition, typical teleostean astroglial cells with small, round bodies mostly on the periventricular or outer surfaces of the brain and long, smooth, thin fibers coursing mainly radially inward were labeled with antibodies against α_{2A}, β_1, and β_2 but not α_{2C} AR. Colocalization with GFAP-specific antibody confirmed the glial identity of those cells.

The most abundant α_2 AR subtype was α_{2A} located in cell bodies and fibers. The overall distribution of α_{2C} AR was low, observed mainly in fibers. Both β_1 and β_2 AR subtypes were widely spread in the teleostean brain and in most cases presented a similar distribution, with β_2 AR predominance. A detailed diagram of the distribution of α_{2A}, α_{2C}, β_1, and β_2 receptor subtypes is presented in Figure 6. Although immunohistochemical labeling is excellent for delineating and elucidating the exact neuroanatomical and cellular distribution of adrenergic receptor subtypes (perikaryal or dendritic subcellular localization and their presence in neuronal and/or glial populations), there are methodological difficulties in quantification of such observations. No apparent changes were detected in the quantitative distribution of each subtype with age or in the numbers or the distributions of immunoreactive elements between the individual animals used.

Telencephalon.

α_{2A}-α_{2C} AR. Dorsal and ventral medial telencephalic areas (Dm1–4, Vv, Vd, Vs) were rich in small α_{2A} AR-ir neurons (Fig. 7A). However, α_{2A} AR-ir was found on astroglial cells as revealed by double labeling with GFAP (Fig. 8A), in the periventricular surfaces of the above-mentioned brain regions along with the outer surfaces of dorsal and lateral regions (Dd, Dld, Dlv, Dll, Dlp). Only

few small α_{2C} AR-ir neurons were detected in the central and lateral part of the ventral telencephalon (Vc, Vl, respectively; Fig. 7B), whereas labeled varicose fibers were observed in central (Dc, Vc), ventrolateral (Vl), and ventromedial (Vv, Vs) regions (Fig. 7B).

β_1-β_2 AR. Telencephalic neuronal populations consisting of medium-sized and small neurons were detected with the β_2 AR antibody mainly in dorsolateral, -medial, and -caudal nuclei as well as the central region (Fig. 7C). A dense network of β_2 AR-ir varicose fibers was located between the lateral and the medial forebrain bundles, whereas β_1 AR-ir varicose fibers were abundant dorsally (Fig. 7D). In the dorsal (Dd, Dm, Dl, Dp) and ventral (Vv, Vl) forebrain, β_1 AR were found in astroglia (Fig. 8C), whereas β_2 AR colocalized with GFAP mainly in Vv (Fig. 8D–F). Autoradiographic studies with the β_1 antagonist BHCl and β_2 antagonist ICI 118551 revealed higher levels of β_2 AR in all dorsal and central regions but equal binding sites in ventromedial areas (Table 2).

Diencephalon.

α_{2A}-α_{2C} AR. Large α_{2A} AR-ir neurons were located in the magnocellular and parvocellular pretectum (PSm, PSp) and magnocellular preoptic nucleus (PMm). Medium-sized neurons were abundant in the dorsal thalamus (DP, CP), preglomerular complex (PGm, PGl; Fig. 9A), hypothalamic inferior lobes (NCILa, NCILp, CE; Fig. 9C), and dorsal hypothalamic area in the vicinity of the lateral recess (nRL, dHA). Smaller neurons were either tightly packed in the posterior tubercle (TPp; Fig. 9A), ventral hypothalamus (Hv), and paraventricular organ (PVO) or diffusely scattered in the inferior lobes (DIF). All those diencephalic areas, including the ventromedial and -lateral thalamus (VM, VL), also contained thin, varicose fibers. The same areas, with the exception of some central inferior lobe nuclei (NCILa, NCILp) and the addition of ventrolateral hypothalamic areas (LH, TA), were rich in α_{2C} AR-ir fibers (Fig. 9B). Few small positive neurons were detected in the parvocellular portion of the preoptic area (PPp), ventral hypothalamus (Hv), and paraventricular organ (PVO). Astroglial cells labeled with α_{2A} AR antibody were sparse and present only in the central periventricular thalamus (Fig. 8B).

β_1-β_2 AR. Both subtypes, especially β_2 AR, colocalize substantially with periventricular glial populations. Thin fibers with varicosities randomly oriented were widely spread and mostly positive for the β_2 AR subtype. The densest AR innervation was observed in the hypothalamus, namely, the preoptic area (β_1 and β_2 AR-ir), lateral tubercle (NDTL; β_1 and β_2 AR-ir), central inferior lobe (CE, NCILp; β_1 and β_2 AR-ir), and lateral recess (nRL; β_2 AR-ir). Pretectal, medial thalamic, and pre- and glomerular nuclei were interspersed with moderate to high densities of axons of both subtypes. Large β_1 AR-ir neurons were found in the anterior preoptic area (PPa), whereas small β_1 AR-ir neurons were scattered in the diffuse hypothalamic nucleus (Fig. 10A). In agreement with the immunohistochemical pattern, autoradiographic studies with β_1 and β_2 antagonists revealed higher β_2 AR densities in all diencephalic areas of the adult teleostean brain (Table 2).

Brainstem and cerebellum.

α_{2A}-α_{2C} AR. Mostly α_{2A} AR-ir fibers were detected in the optic tectum. They were found in both superficial (SO) and deeper (SGFS, SAC) layers, whereas periventricularly (SGP) small, densely packed α_{2A} and α_{2C} AR-ir neurons

TABLE 4. Quantitative Distribution of β AR (fmoles/mg Tissue ± SEM) in Young and Adult Teleosts (Red Porgy, *Pagrus pagrus*)[1]

Area	Age (years)			
	0+	2+	3+	5+
Dorsal telencephalon				
Medial zone 1 of the dorsal telencephalic area (Dm1)	17.5 ± 0.9	12.2 ± 1.9	16.0 ± 7.3	9.4 ± 1.7
Medial zone 2 of the dorsal telencephalic area (Dm2)	16.3 ± 0.6	12.8 ± 1.4	16.1 ± 6.2	9.8 ± 1.9
Medial zone 3 of the dorsal telencephalic area (Dm3)	20.8 ± 1.6	15.2 ± 1.9	19.1 ± 8.2	10.8 ± 2.1[2]
Medial zone 4 of the dorsal telencephalic area (Dm4)	20.3 ± 3.0	14.4 ± 1.6	15.5 ± 6.2	9.8 ± 2.2[2]
Central zone of the dorsal telencephalic area (Dc)	17.7 ± 1.4	11.9 ± 2.3	15.2 ± 9.5	9.9 ± 1.4
Dorsal zone of the dorsal telencephalic area (Dd)	16.5 ± 1.3	11.8 ± 2.0	15.9 ± 9.8	9.7 ± 1.7
Dorsal part of the lateral zone of the dorsal telencephalic area (Dld)	14.0 ± 1.1	16.5 ± 3.7	16.3 ± 4.8	11.0 ± 2.0
Ventral part of the lateral zone of the dorsal telencephalic area (Dlv)	14.9 ± 1.8	17.8 ± 4.3	16.6 ± 5.8	10.9 ± 2.2
Lateral part of the lateral zone of the dorsal telencephalic area (Dll)	15.1 ± 0.9	17.0 ± 2.8	17.8 ± 6.7	11.4 ± 1.4
Posterior part of the lateral zone of the dorsal telencephalic area (Dlp)	18.9 ± 0.8	17.6 ± 4.2	19.0 ± 7.9	12.5 ± 2.5
Posterior zone of the dorsal telencephalic area (Dp)	17.9 ± 1.2	15.9 ± 2.8	17.2 ± 9.8	12.6 ± 2.3
Ventral telencephalon				
Olfactory bulb (OB)	26.8 ± 10.5	11.8 ± 3.3[2]	11.9 ± 6.8[2]	9.5 ± 2.1[2]
Ventral nucleus of the ventral telencephalic area (Vv)	29.5 ± 3.9	14.8 ± 1.7[2]	15.2 ± 4.3[2]	11.3 ± 2.2[2]
Lateral nucleus of the ventral telencephalic area (Vl)	18.3 ± 1.7	17.6 ± 4.1	18.3 ± 6.7	15.3 ± 2.8
Dorsal nucleus of the ventral telencephalic area (Vd)	24.8 ± 2.1	14.7 ± 1.3	13.6 ± 4.8	12.0 ± 2.5[2]
Supracommissural nucleus of the ventral telencephalic area (Vs)	29.7 ± 2.1	15.8 ± 1.8[2]	14.4 ± 4.4[2]	12.0 ± 2.7[2]
Central nucleus of the ventral telencephalic area (Vc)	20.4 ± 2.2	14.8 ± 2.6	16.2 ± 11.0	10.4 ± 1.9[2]
Pretectum				
Superficial pretectal nucleus, parvocellular portion (PSp)	55.1 ± 6.7	28.8 ± 6.7[2]	25.1 ± 12.0[2]	16.5 ± 3.0[2,3]
Superficial pretectal nucleus, magnocellular portion (PSm)	62.1 ± 8.8	26.0 ± 3.1[2]	17.2 ± 3.8[2]	16.3 ± 3.4[2,3]
Dorsal periventricular pretectal nucleus (PPd)	28.5 ± 1.4	18.4 ± 3.1[2]	14.2 ± 5.0[2]	11.7 ± 2.7[2]
Ventral periventricular pretectal nucleus (PPv)	24.6 ± 1.6	17.7 ± 3.5	15.3 ± 5.9	11.8 ± 2.1[2]
Dorsal thalamus				
Habenulla (Ha)	12.4 ± 1.2	8.3 ± 1.9	7.9 ± 5.2	9.2 ± 0.8
Dorsal posterior thalamic nucleus (DP)	21.5 ± 3.8	16.1 ± 3.2	14.3 ± 6.1	11.7 ± 2.7[2]
Central posterior thalamic nucleus (CP)	25.6 ± 2.4	15.4 ± 3.6[2]	13.6 ± 7.4	11.1 ± 2.4[2]
Ventral thalamus				
Ventromedial nucleus (VM)	25.1 ± 2.0	16.8 ± 3.3	12.4 ± 6.3[2]	11.5 ± 2.3[2]
Ventrolateral nucleus (VL)	27.9 ± 3.2	14.7 ± 3.6[2]	15.1 ± 10.9[2]	10.3 ± 1.9[2]
Periventricular nucleus of the posterior tuberculum (TPp)	20.4 ± 2.1	13.9 ± 2.9	13.2 ± 6.1	12.3 ± 2.1
Pre-/glomerular complex				
Medial preglomerular nucleus (PGm)	35.8 ± 2.2	22.5 ± 2.0[2]	15.0 ± 4.1[2]	18.1 ± 4.0[2]
Lateral preglomerular nucleus (PGl)	43.5 ± 4.6	23.9 ± 4.4[2]	24.3 ± 15.1[2]	18.0 ± 3.4[2]
Glomerular nucleus (G)	30.0 ± 4.0	13.9 ± 3.1[2]	13.7 ± 8.2[2]	11.1 ± 1.6[2]
Preoptic area				
Medial magnocellular preoptic nucleus (PMm)	26.3 ± 0.7	15.6 ± 3.4[2]	13.0 ± 5.2[2]	13.6 ± 1.4[2]
Posterior parvocellular preoptic nucleus (PPp)	18.1 ± 2.4	12.4 ± 1.7	12.4 ± 5.1	11.1 ± 2.3
Anterior parvocellular preoptic nucleus (PPa)	25.5 ± 2.7	16.6 ± 1.7	12.9 ± 5.0[2]	10.0 ± 2.0[2]
Suprachiasmatic nucleus (SC)	20.2 ± 5.2	13.6 ± 1.7	10.9 ± 6.3	9.6 ± 0.9[2]
Dorsal hypothalamus				
Dorsal hypothalamic area (dHA)	20.9 ± 3.9	15.3 ± 2.5	13.8 ± 6.2	11.8 ± 1.7
Nucleus of the lateral recess (nRL)	15.9 ± 3.8	15.3 ± 2.5	13.8 ± 6.2	11.7 ± 1.8
Paraventricular organ (PVO)	28.1 ± 2.6	16.2 ± 2.8[2]	12.5 ± 5.8[2]	13.1 ± 2.3[2]
Anterior tuberal nucleus (TA)	18.6 ± 1.2	15.0 ± 1.1	12.1 ± 6.5	11.1 ± 1.5
Mammillary corpus (CM)	23.1 ± 1.2	15.2 ± 3.1	11.7 ± 5.7	12.8 ± 2.5[2]
Ventral hypothalamus				
Lateral tuberal nucleus (nLT)	15.8 ± 1.6	15.7 ± 3.3	15.8 ± 3.7	13.5 ± 2.1
Nucleus of the lateral hypothalamus (LH)	20.3 ± 1.5	14.6 ± 2.2	15.4 ± 8.9	12.1 ± 2.0
Nucleus of the periventricular ventral hypothalamus (Hv)	24.5 ± 1.5	14.1 ± 3.4[2]	15.2 ± 6.7	12.3 ± 2.3[2]
Nucleus of the periventricular caudal hypothalamus (Hc)	14.8 ± 1.8	18.9 ± 1.6	19.5 ± 7.3	17.2 ± 4.5
Lateral torus-inferior lobe				
Diffuse nucleus of the lateral torus (NDTL)	51.6 ± 7.3	24.3 ± 5.4[2]	23.9 ± 11.6[2]	14.5 ± 2.3[2,3]
Anterior nucleus of the central part of the inferior lobe (NCILa)	53.5 ± 8.5	27.2 ± 5.9[2]	21.6 ± 11.0[2]	15.2 ± 3.6[2,3]
Posterior nucleus of the central part of the inferior lobe (NCILp)	39.0 ± 3.2	25.0 ± 4.1[2]	25.3 ± 11.7[2]	15.8 ± 2.8[2]
Central nucleus of the inferior lobe (CE)	18.6 ± 1.4	12.6 ± 2.4	11.4 ± 7.7	10.2 ± 2.1
Diffuse nucleus of the inferior lobe (DIF)	15.3 ± 3.4	12.8 ± 2.1	14.2 ± 7.5	10.2 ± 1.9
Optic tectum				
Stratum opticum (SO)	6.5 ± 0.5	6.9 ± 1.8	5.1 ± 2.7	5.7 ± 0.4
Stratum griseum centrale (SGC)	10.8 ± 1.4	13.0 ± 2.7	10.4 ± 7.0	9.5 ± 1.3
Stratum fibrosum et griseum superficiale (SGFS)	16.6 ± 2.2	14.3 ± 3.2	9.4 ± 5.7	8.7 ± 1.3
Stratum griseum periventriculare (SGP)	15.2 ± 2.7	16.5 ± 2.2	14.6 ± 8.6	11.4 ± 1.7
Stratum album centrale (SAC)	4.9 ± 1.2	4.8 ± 1.5	4.0 ± 1.8	3.8 ± 1.2
Semicircular torus				
Semicircular torus, layer 1 (TS1)	14.5 ± 1.0	11.8 ± 2.7	6.8 ± 1.3	8.7 ± 1.5
Semicircular torus, layer 2 (TS2)	18.7 ± 2.6	14.1 ± 2.5	13.8 ± 5.2	9.8 ± 1.7
Semicircular torus, layer 3 (TS3)	14.6 ± 5.1	10.7 ± 3.0	8.5 ± 5.2	8.4 ± 0.8
Semicircular torus, layer 4 (TS4)	21.9 ± 5.0	15.2 ± 3.6	11.5 ± 6.1	11.6 ± 2.0[2]
Isthmic area-midbrain tegmentum				
Locus coeruleus (LoC)	41.4 ± 7.5	15.6 ± 3.2[2]	14.5 ± 5.7[2]	11.4 ± 1.9[2]
Isthmic nucleus (is)	36.8 ± 4.8	20.4 ± 2.1[2]	16.6 ± 3.5[2]	15.7 ± 2.7[2]
Cortical nucleus (NC)	35.6 ± 7.9	24.9 ± 5.1[2]	15.7 ± 8.4[2]	18.3 ± 3.2[2]
Nucleus of the medial longitudinal fascicle (nuflm)	35.2 ± 4.7	19.9 ± 4.0[2]	12.6 ± 6.8[2]	11.8 ± 2.1[2]
Medial longitudinal fascicle (flm)	10.2 ± 3.6	11.0 ± 2.8	9.2 ± 6.8	7.9 ± 0.9
Oculomotor nucleus (NIII)	33.2 ± 4.9	20.7 ± 5.1[2]	13.3 ± 2.4[2]	12.8 ± 2.1[2]
Central grey (GC)	23.8 ± 6.9	14.1 ± 3.6	8.0 ± 3.9[2]	9.9 ± 1.5[2]
Dorsal raphe (Rd)	30.3 ± 9.4	21.6 ± 4.2	13.5 ± 6.2[2]	12.5 ± 2.2[2]
Medial raphe (Rm)	29.4 ± 8.8	20.1 ± 4.0	14.1 ± 6.2[2]	12.5 ± 2.5[2]
Interpeduncular nucleus (NIn)	27.9 ± 7.6	18.6 ± 3.2	15.6 ± 5.5	13.2 ± 2.8[2]
Motor nucleus of the trigeminal nerve (NVm)	43.2 ± 7.8	22.5 ± 4.7[2]	15.1 ± 8.3[2]	13.2 ± 2.9[2]
Inferior reticular nucleus (ri)	35.4 ± 7.6	24.0 ± 5.6[2]	12.4 ± 7.0[2]	10.8 ± 2.2[2]
Medial reticular nucleus (rm)	33.1 ± 7.0	20.8 ± 4.5[2]	13.6 ± 9.1[2]	13.4 ± 2.4[2]
Superior reticular nucleus (rs)	38.9 ± 8.0	25.5 ± 5.1[2]	14.6 ± 8.6[2]	13.9 ± 2.5[2]
Inferior olive (oli)	33.4 ± 6.3	21.2 ± 3.3[2]	15.8 ± 10.1[2]	12.4 ± 2.0[2]

TABLE 4. (continued)

Area	Age (years)			
	0+	2+	3+	5+
Cerebellum-accessory cerebellar nuclei				
Longitudinal torus (tlo)	28.2 ± 3.2	14.1 ± 2.9^2	14.0 ± 4.4^2	13.0 ± 2.2^2
Nucleus of the lateral valvula (lv)	22.4 ± 1.9	16.3 ± 3.4	15.1 ± 6.9	12.1 ± 2.7
Lateral granular eminence (Egl)	24.6 ± 1.2	18.1 ± 3.6	17.1 ± 7.3	12.9 ± 1.6^2
Medial granular eminence (Egm)	27.6 ± 2.8	19.5 ± 4.8	12.7 ± 4.7^2	14.9 ± 3.2^2
Granular layer of the valvular cerebelli (VCbgr)	15.7 ± 1.5	10.4 ± 1.9	9.2 ± 5.7	10.6 ± 2.0
Molecular layer of the valvular cerebelli (VCbmol)	23.4 ± 3.0	19.1 ± 4.1	17.8 ± 10.0	18.3 ± 3.4
Granular layer of the cerebellar corpus (CCbgr)	13.2 ± 3.8	11.0 ± 2.7	11.1 ± 5.9	10.0 ± 2.7
Molecular layer of the cerebellar corpus (CCbmol)	19.3 ± 5.8	16.8 ± 3.2	23.3 ± 9.9	13.9 ± 4.4
Medial proliferation zone of the cerebellar corpus (CCbPZ)	42.5 ± 7.7	26.2 ± 3.2^2	36.8 ± 15.0	24.5 ± 8.1^2
Overall	15.2 ± 2.4	8.5 ± 2.0	9.6 ± 4.9	7.9 ± 1.4

[1]Footnotes 2 and 3 highlight significant differences (one-way ANOVA, dependent factor: receptor density, independent factor: age, $P < 0.05$, LSD Post-Hoc test).
[2]Significant difference with the age 0+.
[3]Significant difference with the age 2+.

were observed (Fig. 9D). The semicircular torus exhibited labeled fibers of both subtypes as well as small and medium-sized α_{2A} AR-ir neurons in the second and fourth layers. Right below the tectum, the cortical nucleus (NC) consisted of large, tightly packed neurons labeled with both AR subtypes. In the isthmal area, only α_{2A} AR-ir was detected, with small neurons forming a cluster in the isthmic nucleus and larger neurons appearing in locus coeruleus (Fig. 9E). Labeled fibers were present in both areas. Rostrally in the dorsomedial tegmentum, large neurons (α_{2A} and α_{2C} AR-ir), medium-sized neurons (α_{2A} AR-ir), and fibers of both subtypes were observed in nuclei of tracts (nuflm) and nerves (NIII). The central gray (GC) contained small and medium-sized α_{2A} AR-ir neurons, but α_{2C} AR-ir fibers. More caudally, α_{2C} AR immunoreactivity was confined to fibers colocalizing with α_{2A} AR-ir fibers in the raphe complex (Rd, Rm), interpeduncular nucleus (NIn), reticular formation (rs, ri, rm; Fig. 9F), and nucleus of the trigeminal nerve (NVm). All these areas except for NIn displayed large and medium-sized α_{2A} AR-positive neurons. Finally, in the cerebellum, only the Purkinje cell layer was lightly positive for α_{2A} and α_{2C} AR.

β_1-β_2 AR. Mostly β_2 AR immunoreactivity colocalized with astroglia, mainly around the periphery and midline of the brain (Fig. 8H,K). The main noradrenergic center, LoC, consisted of large β_1 and β_2 AR-ir neurons and β_2 AR-ir fibers (Figs. 8H, 9C,D). A similar pattern but with small β_1 AR-ir neurons was observed in the central gray (GC). Apart from that, both subtypes shared a common distribution pattern: localized in small neurons and dendrites of the optic tectum (SGP; Fig. 10B) and the semicircular torus (TS2, TS4), large and medium-sized neurons of the rostral (nuflm, NS, NIII) and caudal (Rd, Rm, NIn, ri, rs, rm) tegmentum (Fig. 10E), and fibers located either in tracts (flm) or widely spread, often mediolaterally oriented along the mesencephalic tegmentum.

In the cerebellum and accessory cerebellar structures (tlo, lv; Figs. 8J,K, 9F), both β_1 and β_2 AR-ir in cell bodies and fibers were considerably high, particularly in the Purkinje cell layer and the molecular layer. Purkinje cells and their dendrites were labeled so intensely that it was impossible to detect any other (e.g., glial) immunoreactive fibers in the double-labeling experiments. Subtype-specific autoradiographic studies revealed a consistently higher density of the β_2 AR binding sites compared with the β_1 binding in all brainstem regions and cerebellum (Table 2).

DISCUSSION
Properties of adrenergic receptors in the teleostean brain

Our results demonstrate that fish α_2 and β AR have characteristics similar to those of corresponding amphibian (Herman et al., 1996), avian (Dermon and Kouvelas, 1988; Ball et al., 1989; Fernandez-Lopez et al., 1997), and mammalian (Palacios and Kuhar, 1980; Pazos et al., 1985; Unnerstall et al., 1985) receptors. For the first time, a detailed quantitative distribution of α_2 and β AR in developing and adult teleost brain is provided, by using [3H]clonidine for the determination of α_2 AR and [3H]DHA for β AR. Saturation kinetic studies performed on tissue sections have indicated that binding of both ligands is saturable and of high affinity, with one binding site for each compound. The concentrations of the radioligands used were in the range of those reaching the B_{max} plateau and, of the cold drugs, in the range of maximal inhibition on binding of the respective radioactive ligand. Dissociation constant (K_d) values were in all cases in the nanomolar range, similar to those reported for other vertebrate species (Unnerstall et al., 1985; Dermon and Kouvelas, 1988; Herman et al., 1996). However, maximal receptor densities (B_{max}) in most areas were considerably lower than those reported for birds (Dermon and Kouvelas, 1988) and mammals (Palacios and Kuhar, 1980; Unnerstall et al., 1985), in studies with the same ligands. This could reflect a difference in brain noradrenaline concentrations, as suggested for similar differences between quails and rats (Ball et al., 1989). Indeed, plasma noradrenaline levels in teleosts are higher than those in land vertebrates (Finkenbine et al., 2002). In addition, adrenaline is suggested to be the major transmitter substance in autonomic adrenergic neurons in teleost fish (Holmgren and Nilsson, 1982), as well as in frog brain (Cooney et al., 1985), in accordance with the comparable AR levels in teleost and frog (Herman e al., 1996) central nervous system. However, one cannot rule out the possibility that the observed differences in comparison with avian and mammalian data are, at least partially, related to different pharmacological characteristics of the fish AR. Indeed, studies on skin and peripheral organ AR in fish have reported unique pharmacological properties (Holmgren and Nilson, 1982; Karlsson et al., 1989), and cloning of α_2 AR, though pointing out significant similarities of that receptor and its mammalian counterparts, suggested that
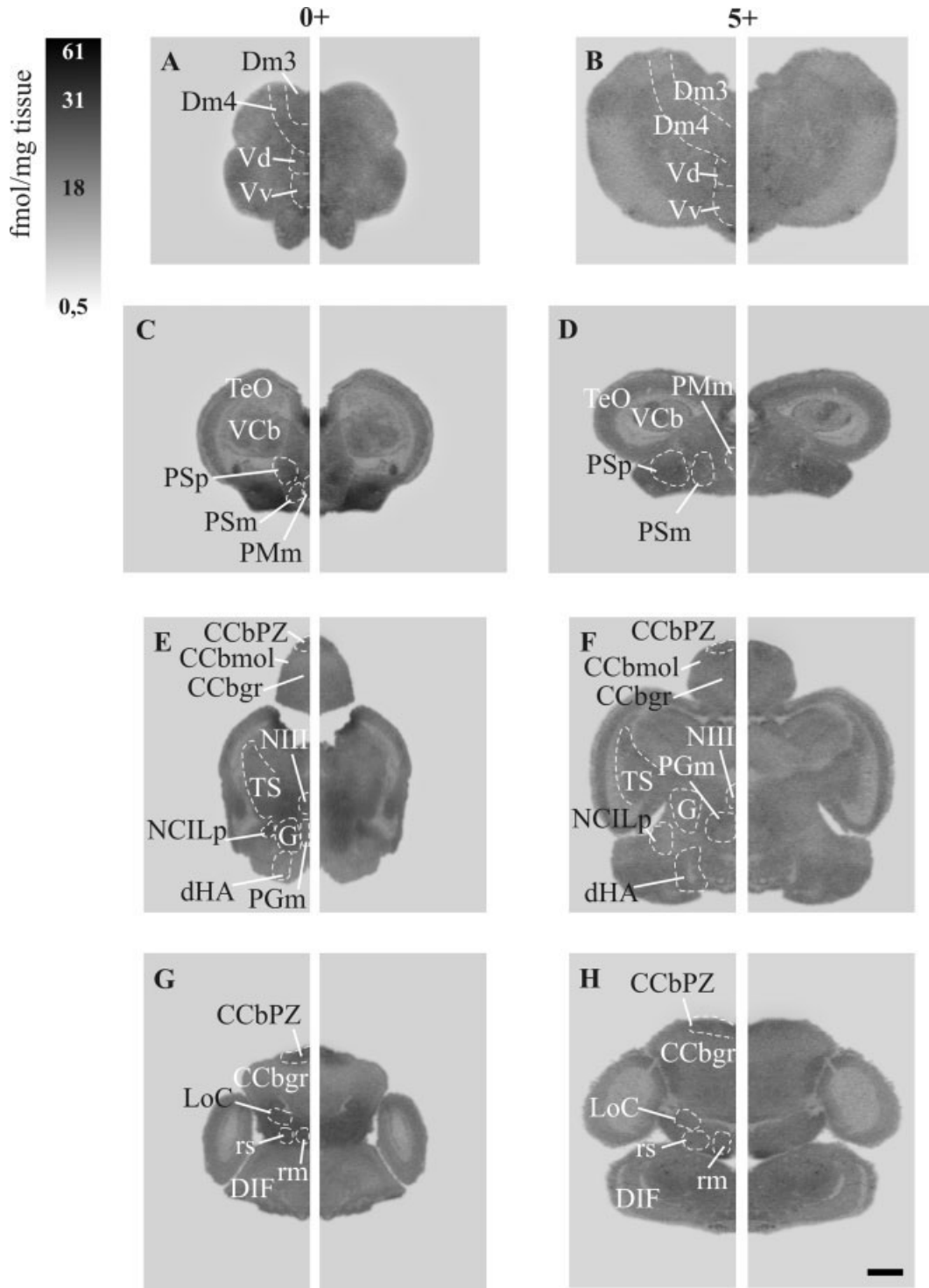
Fig. 4. Autoradiographic images of coronal sections in prosencephalic (A,B), midbrain (C,F), and hindbrain (G,H) regions of young (0+; **A,C,E,G**) and adult (5+; **B,D,F,H**) red porgies, showing the regional density of β adrenoceptors and the alterations during development (for details and abbreviations see text and Table 4). The levels of β receptors decrease with age in most brain regions. Scale bar = 2,000 μm in H (applies to A–H).
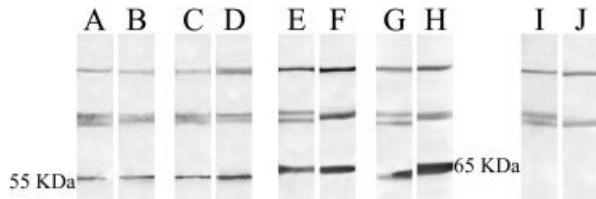
Fig. 5. Antibodies directed against mammalian adrenoceptors recognize the homologous proteins from red porgy. Lanes A,B: Western blots prepared from red porgy (A) and rat (B) brain homogenates were reacted with polyclonal antimammalian α_{2A} AR antibody. Lanes C,D: Western blots prepared from red porgy (C) and rat (D) brain homogenates were reacted with polyclonal antimammalian α_{2C} AR antibody. Lanes E,F: Western blots prepared from red porgy (E) and rat (F) brain homogenates were reacted with polyclonal antimammalian β_1 AR antibody. Lanes G,H: Western blots prepared from red porgy (G) and rat (H) brain homogenates were reacted with polyclonal antimammalian β_2 AR antibody. Lanes I,J: Negative controls prepared from red porgy (I) and rat (J) brain homogenates with the omission of primary antibodies. In all cases, note the stronger expression of adrenoceptor proteins in rat brain, which is in agreement with the observed lower levels of receptors in teleostean brain.

it might represent an ancestral α_2 AR subtype (Svensson et al., 1993), highly correlated with a frog α_2 AR (Herman et al., 1996). Moreover, recent cloning and mapping of zebrafish α_2 AR indicates conservation of α_2 AR subtypes across species (Ruuskanen et al., 2004). Similarly, the β AR gene family is conserved in such evolutionarily divergent species as fish and mammals, and phylogenetic analysis revealed that rainbow trout β AR sequence is most closely related to mammalian β_2 AR (Nickerson et al., 2001), in agreement with the frog β_2 AR subtype suggested to be a primitive form of β AR (Nahorski, 1978).

With the use of receptor subtype-specific antibodies (α_{2A}, α_{2C}, β_1, β_2) and antagonists (BHCl, ICI 118,551), we clearly showed the existence of receptor subtypes in the teleost brain, their neuronal and glial localization, and their differential distribution pattern in various brain areas. It should be noted that the polyclonal AR subtype-specific antibodies used have been tested only in mammals. However, several pieces of evidence indicate that all the polyclonal antibodies used, directed against mammalian adrenergic receptor forms, possibly recognize the teleostean homologues of α_{2A}, α_{2C}, β_1, and β_2 receptors. Western blots of red porgy brain exhibited the same molecular weight protein bands as the respective rat AR, suggesting that the teleostean and mammalian receptors share at least a few conserved epitopes recognized by those antibodies. All antibodies used have been raised to recognize C-terminus receptor domains. Even though studies on mammalian adrenergic receptors indicate a certain degree of diversity for those domains (Kobilka, 1992), molecular studies on fish skin α_2 AR have shown that the greatest identity of fish and mammalian α_2 AR is in the membrane-spanning and intracellular domains, which are thought to be evolutionarily conserved (Svensson et al., 1993). In addition, as in earlier studies (Aoki et al., 1987, 1994), the lack of labeling following preadsorption of the primary antibodies with the peptides used to raise those antibodies in mammals suggests that the antibodies recognized a protein fraction common for α_2, β_1, and β_2 AR in mammals and teleost brain.

The distribution of immunoreactivity for each antibody is well correlated with the corresponding ligand binding density in each brain area. Specifically, for β AR, the observed immunoreactivity is in accordance with the specific β_1 and β_2 AR binding results. Even though further work is needed to confirm the applicability of the α_{2A}/α_{2C} and β_1/β_2 AR terminology in fish, we propose based on our results that α_{2A} and β_2 AR are predominant in the teleostean brain. With respect to α_{2A} AR, this is in agreement with results obtained in amphibian (Herman et al., 1996), avian (Dermon and Kouvelas, 1988; Fernandez-Lopez et al., 1997), and some mammalian (DeVos et al., 1992; Ordway et al., 1993; Uhlen et al., 1997) brains. As concerns β AR, our proposal for β_2 AR predominance is in agreement with studies in frog brain (Nahorski, 1978; Herman et al., 1996) and some observations in avian species (Fernandez-Lopez et al., 1997; Revilla et al., 1998) but is contradicted by studies on human and rat brains (Palacios and Kuhar, 1980; Pazos et al., 1985) that pinpoint β_1 as the predominant subtype.

Distribution and cellular specificity of α_2 and β AR: association with noradrenergic innervation

Our results show a widespread distribution of α_2 and β AR in the teleost brain, as expected from the presence of noradrenergic innervation in all vertebrates (for review see Smeets and Gonzalez, 2000). Most areas included both α_2 and β AR, suggesting their complementary role in noradrenergic function, possibly related to their neuronal and/or glial localization as well as their subcellular specialization (pre-, postsynaptic). Immunocytochemical studies in mammals have provided evidence that the A subtype of α_2 AR is found both at presynaptic and at postsynaptic sites (Aoki et al., 1994). Autoradiographic localization of receptors does not differentiate between pre- and post synaptic sites, although the immunocytochemical localization clearly defined their neuronal (dentritic, perikaryal) or astrocytic topography. However, perikaryal localization of receptors may indicate their postsynaptic or presynaptic site, the latter possibly indicating receptor proteins that are transported to the terminals. The correlation of AR topography with the noradrenergic innervation in specific regions may provide some partial evidence favoring their pre- or postsynaptic localization or both. Teleostean noradrenergic innervation has been described in detail (Ekström et al., 1986; Meek et al., 1993; Ma, 1994a,b, 1997), so the association of receptor binding with noradrenaline levels will be, unless otherwise stated, based on these studies.

In general, receptor distribution and binding levels corresponded well to noradrenergic innervation; e.g., known densely innervated areas were found to be rich in receptors. This positive correlation was characteristically depicted in the dorsal telencephalon and hypothalamus, where moderate to high levels of AR were correlated with dense noradrenergic innervation. In addition, multisensory integration centers (such as the optic tectum and the semicircular torus), most midbrain tegmentum, and accessory cerebellar and cerebellar regions included high β AR binding sites, in accordance with their noradrenergic innervation. In contrast, ventral forebrain known to receive very low and sparse noradrenergic innervation, mainly in central regions, exhibited high AR binding levels (with α_2 AR binding consistently higher than that of β AR), in accordance with the immunocytochemical localization of
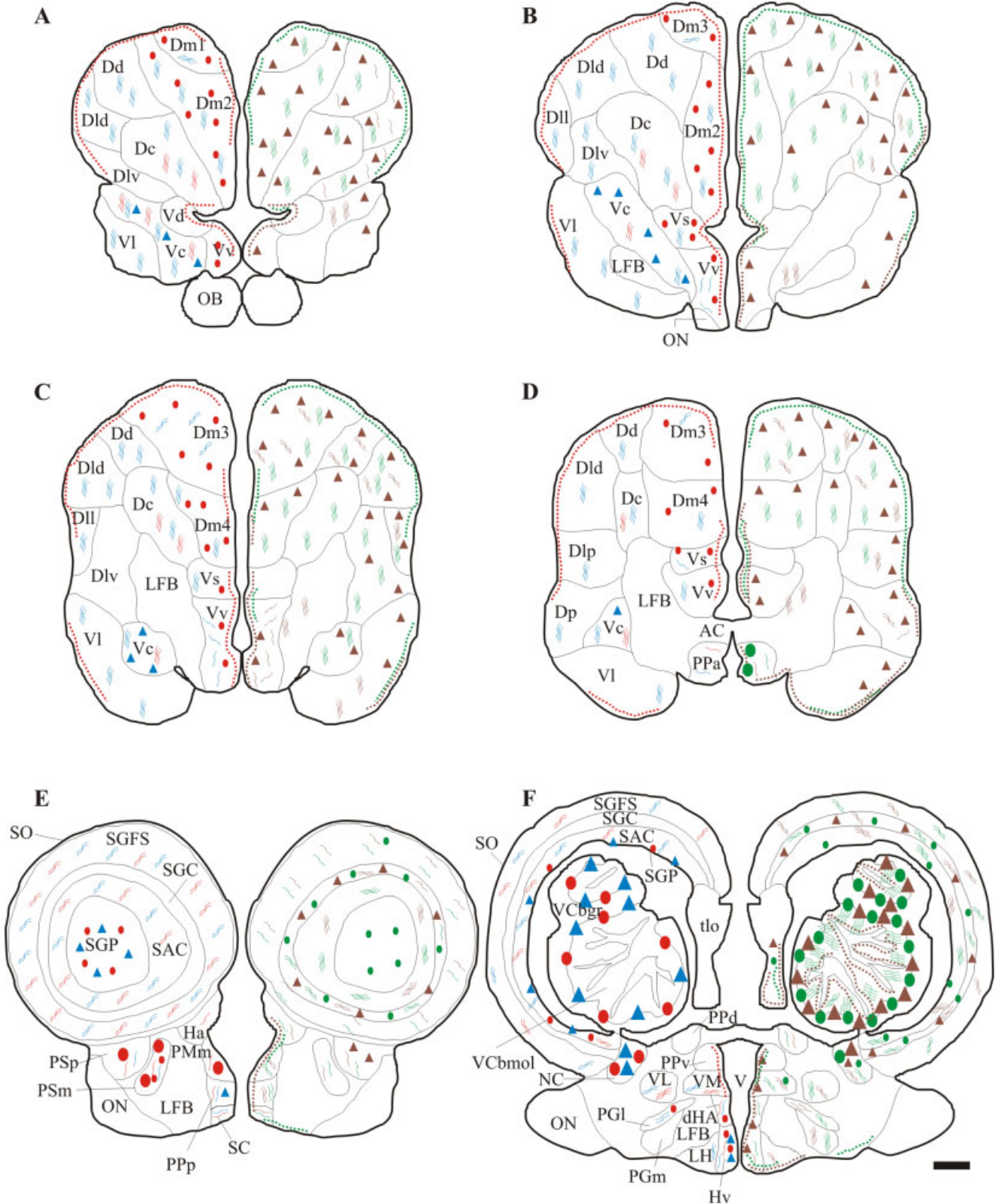
Fig. 6. Outlines from digitized images of transverse sections depicting the distributions of α_{2A}-ir and α_{2C}-ir (left hemisphere) and of β_1-ir and β_2-ir (right hemisphere) cells and fibers in the brain of an adult Sparidae teleost. **A–D:** Telencephalon. **E,F:** Rostral diencephalon and mesencephalon. **G,H:** Central diencephalon and mesencephalon. **I–L:** Caudal diencephalon, mesencephalon, and brainstem. Large dots and triangles represent large neurons, whereas smaller dots and triangles represent medium-sized and small neurons. Dotted lines indicate positive glial cell bodies and fibers. Curved lines indicate varicose fibers. Red, blue, green, and brown shapes and lines correspond to α_{2A}, α_{2C}, β_1, and β_2 immunoreactivity, respectively. For details and abbreviations see text and tables. Scale bars = 1,000 μm in F (applies to A–F), L (applies to G–L).
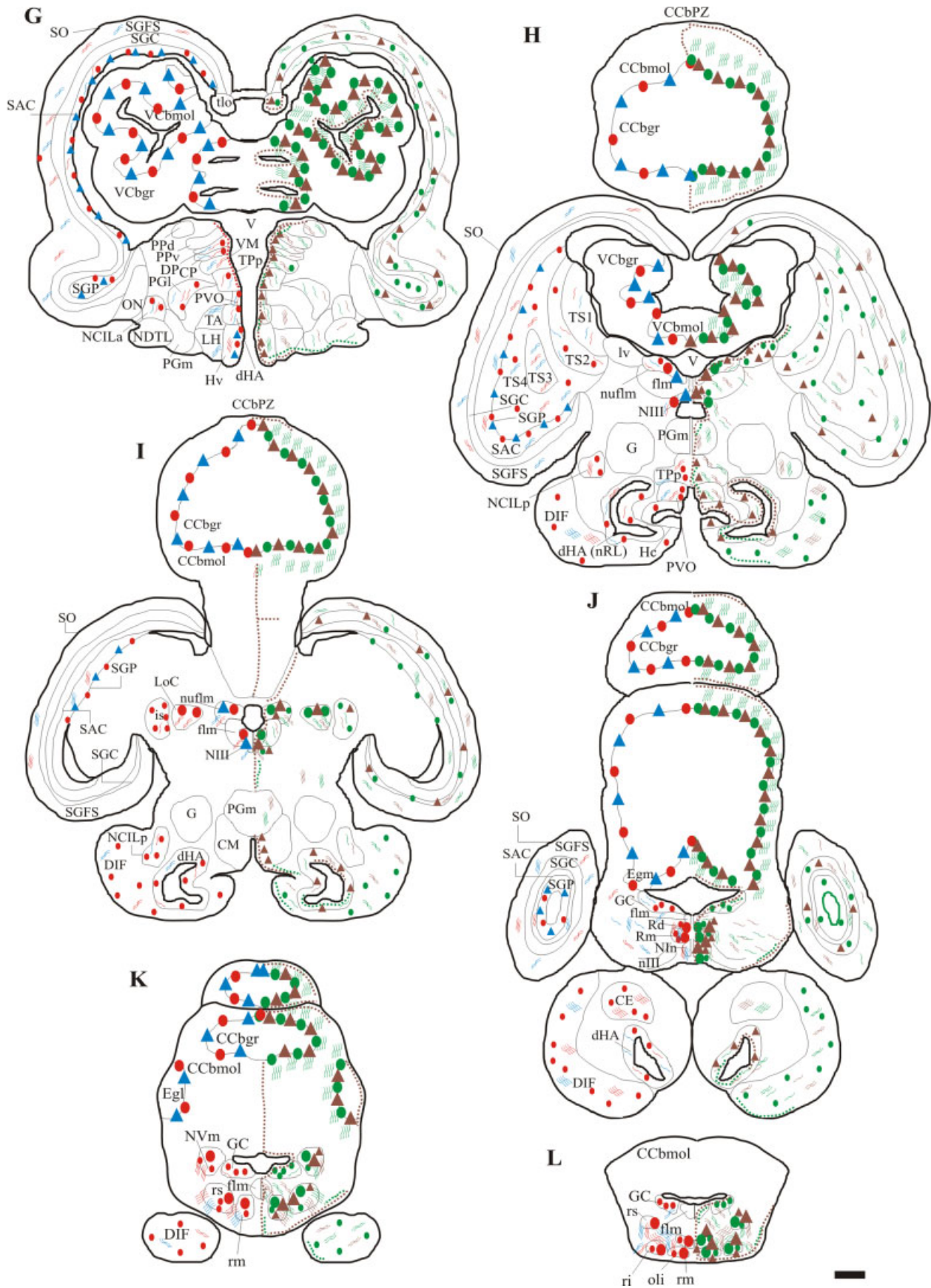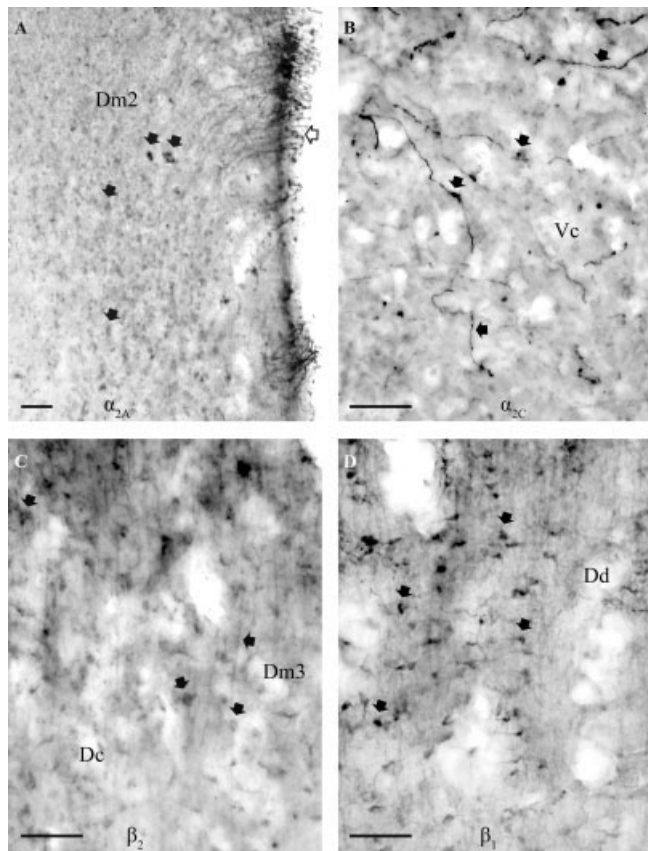
Fig. 6. (continued)

Fig. 7. Photomicrographs of telencephalic coronal sections showing the distribution of adrenergic receptor subtypes (**A:** α_{2A}; **B:** α_{2C}; **C:** β_2; **D:** β_1). Solid arrows indicate neuronal somas and fibers; open arrow highlights α_{2A}^+ glial cells (for details and abbreviations see text and tables). Scale bars = 100 μm.

all receptor subtypes in small and medium-sized neurons and fibers. Mismatches of the localization of AR and noradrenergic innervation included the pretectum, posterior tubercle, and pre-/glomerular complex. In the thalamus, receptor autoradiography showed moderate α_2 and β receptor levels well correlated with the presence of varicose fibers expressing all subtypes and neuronal populations expressing β_1 and α_{2A} AR-ir, the latter following the distribution of dopaminergic neurons (Kaslin and Panula, 2001). All those areas, with the exception of the pre-/glomerular complex, receive dense dopaminergic innervation (Kaslin and Panula, 2001), suggesting possible noradrenergic–dopaminergic system interactions. Studies on teleosts have shown the close interaction of the dopaminergic and noradrenergic systems, pointing out that most noradrenergic neurons are also dopaminergic (Meek et al., 1993; Smeets and Gonzalez, 2000; Kaslin and Panula, 2001), supporting the possible localization of adrenergic receptors on dopaminergic neurons. Similar discrepancies found in mammalian brain regions are also implying a complex relationship between noradrenaline and dopamine through which the noradrenergic system facilitates dopaminergic neurotransmission by mediating the release or synthesis of dopamine (Uhlen et al., 1997).

The origin of the noradrenergic system, LoC, located in the isthmal region just rostral to the motor nucleus of the

trigeminal nerve and lateral to the medial longitudinal fascicle, included a cluster of large, unipolar and bipolar neurons (α_{2A}, β_1, β_2 positive) with dendrites extending ventrolaterally (which are β_1 and β_2 positive). It exhibited the highest levels of α_2 AR binding. A comparable group of cells has been identified in a number of teleosts and has been implicated in the noradrenergic innervation of most brain areas (Ekström et al., 1986; Brantley and Bass, 1988; Sas et al., 1990; Meek et al., 1993; Ma, 1994a; Kaslin and Panula, 2001). Most likely the majority of the receptors observed in LoC function as presynaptic autoreceptors, regulating noradrenergic output, when they are transported to the cell terminals. The isthmal and medullar brain regions that receive dense noradrenergic input exhibited moderate to high receptor levels and contained the highest number of immunoreactive fibers and neurons of all receptor subtypes.

Glial cells expressed β_2, α_{2A}, and β_1 subtypes, even though the colocalization of the α_{2A} and β_1 AR subtypes with GFAP immunoreactivity is not as extensive as in the case of β_2 AR, accounting for a significant portion of the overall receptor density. It is therefore suggested that the predominance of β_2 AR in the teleost brain is partially related to the extensive localization on astroglial cells. Glial cell complexity in the teleostean brain has been described in detail elsewhere (Kalman, 1998; Forlano et al., 2001; Zupanc and Clint, 2003), and our results further support its significance in fish brain. In agreement, AR are found in glial cells in mammals (Köster, 1995; Hodges-Savola et al., 1996; Wang and Lidow, 1997; Milner et al., 1998), and mammalian astrocytes also express the β_2 AR subtype (Mantyh et al., 1995). The presence of AR in teleost astrocytes points out the conservation of their glial in addition to their neuronal localization in the phylogenetically distant teleosts.

Regional pattern in AR development

The present study provides quantitative anatomical details of the postnatal α_2 and β AR system in the developing teleostean brain. Saturation analysis of receptor binding between younger and older animals resulted in curves with similar slopes, indicating that the affinity of the receptors did not change with age, in accordance with developmental studies in other vertebrates (Dermon and Kouvelas, 1988; Happe et al., 2004). Therefore, our results clearly indicate that changes in receptor levels at different ages are due to changes in the number of binding sites, although we cannot safely postulate on the functional consequences regarding their synaptic efficacy. Although most areas included both α_2 and β AR, suggesting their complementary role in noradrenergic function, the developmental course of adrenergic receptors was region and type specific. Many areas included levels similar to adult levels throughout the stages studied of one or both receptor types, indicating an early maturation pattern. The rest of the brain areas included the highest AR levels, higher than adult levels, at the earliest stage studied, between 6 and 12 months of age (0+), clearly suggesting a potential developmental role for α_2 and β AR. Selective regional decreases, transient or not, characterized all cases of the β AR changes, and most of the observed α_2 AR alterations. In agreement with this, overall β_1 (Sastre et al., 2001) and β_2 (Weiland and Wise, 1986) AR densities decline when mammals or birds mature following initial increases of β AR receptor binding sites early in life (Pittman et al.,
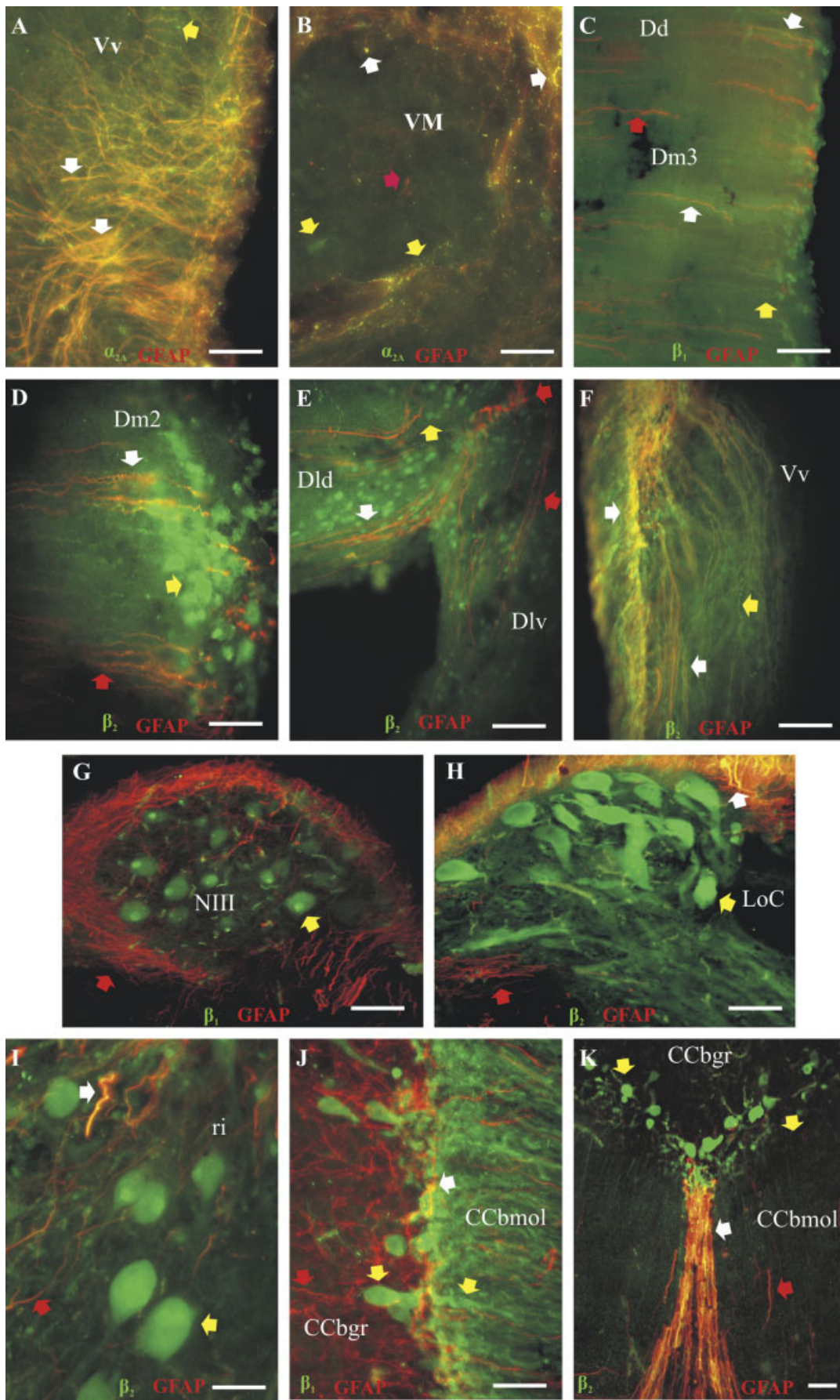
Fig. 8. Photomicrographs showing the distribution of glial cells (GFAP; red fluorescence and red arrows) and the colocalization with α_{2A}, β_1, and β_2 adrenoceptors (green fluorescence and yellow arrows) in the telencephalon (**A:** α_{2A}; **C:** β_1; **D–F:** β_2), thalamus (**B:** α_{2A}), brainstem (**G:** β_1; **H,I:** β_2) and cerebellum (**J:** β_1; **K:** β_2). White arrows and yellow fluorescence indicate double-labeled glial cells and fibers (for details and abbreviations see text and tables). Scale bars = 100 μm.
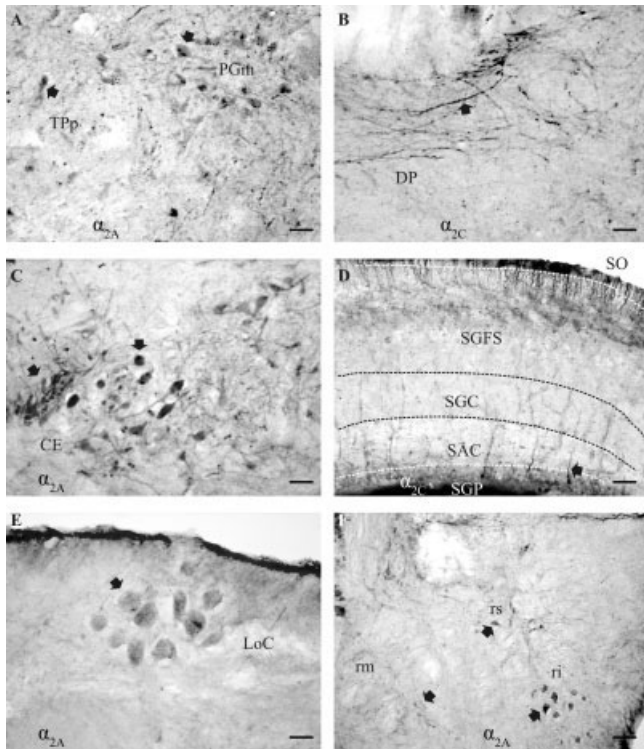
Fig. 9. Photomicrographs of thalamic (**A,B**), hypothalamic (**C**), optic tectum (**D**), and brainstem (**E,F**) coronal sections showing the distribution of α_2 adrenergic receptor subtypes (A,C,E,F: α_{2A}; B,D: α_{2C}). Arrows indicate neuronal somas and fibers (for details and abbreviations see text and tables). Scale bars = 100 μm in A–E; 200 μm in F.
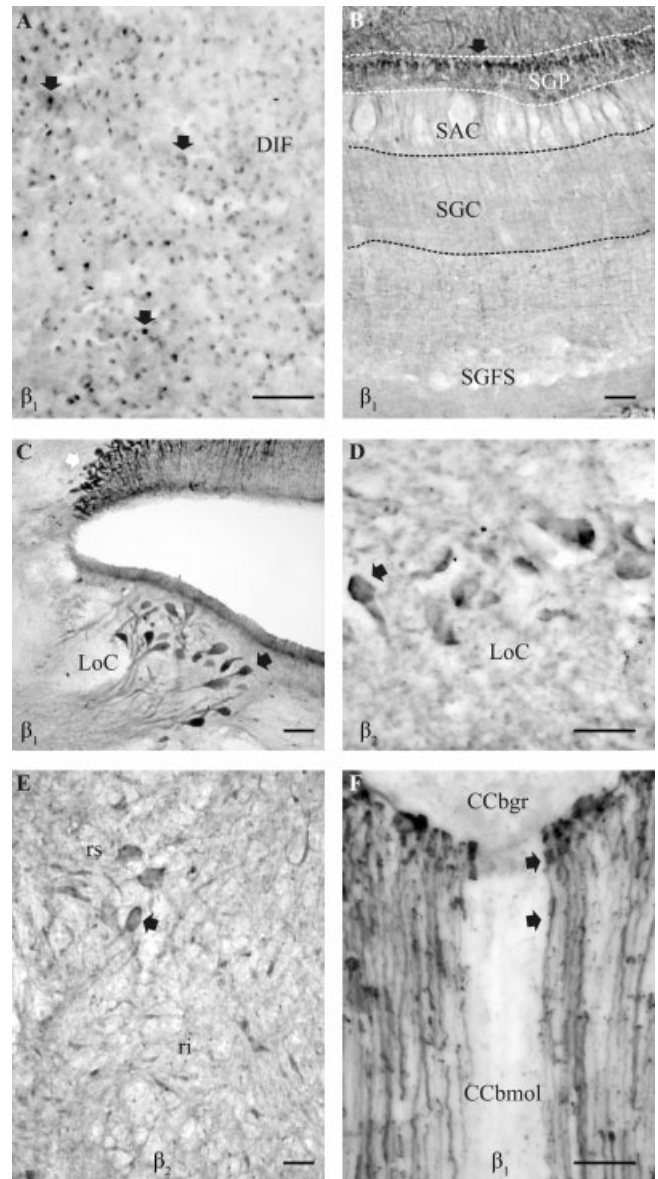

Fig. 10. Photomicrographs of hypothalamic (A), tectal (B), and brainstem (C,F) coronal sections showing the distribution of β adrenergic receptor subtypes (A–C,F: β_1; D,E: β_2). Black arrows indicate neuronal somas and fibers; white arrows in C and arrowheads in F highlight Purkinje cells (for details and abbreviations see text and tables). Scale bars = 100 μm in A,B,D–F; 200 μm in C.

1980; McDonald et al., 1982; Lorton et al., 1988; Dermon and Kouvelas 1988). The use of specific β_1 and β_2 AR antagonists revealed the predominance of the β_2 subtype and demonstrated that in most cases decreases in β AR densities with age were due mainly to the pronounced loss of β_1 AR binding sites, insofar as β_2 AR remained unchanged or decreased slightly at a very slow rate. Specifically for α_2 AR, selected areas, such as SAC of optic tectum, nucleus of lateral valvula, and granular layer of cerebellar corpus, expressing negligible levels in adult, transiently expressed moderate levels of receptors at 0+ stages, in agreement with developmental studies in mammals (Happe et al., 2004) and birds (Dermon and Kouvelas, 1988). Decreases in α_2 receptors with age were also reported for mammalian forebrain (thalamic, hypothalamic, and telencephalic) areas (Hamilton et al., 1984; Mishra et al., 1985; Pascual et al., 1991) and cerebellum (Flügge et al., 1993).

The observed decreases in the density of AR could indicate actual decreases in the number of synaptic contacts or, alternatively, increases in other neuronal or glial elements not associated with the receptors under study (cell bodies becoming larger, neuropil becoming denser, glial elements increasing, etc.). If the latter were the case, synaptic efficacy would remain constant, with a reduction of receptor relative density. The significant decline of α_2 and β AR levels in LoC with age favors the synapse-elimination hypothesis, insofar as teleostean LoC provides

most, if not all, of the noradrenergic innervation of the brain rostral to the isthmus, much as it does in other vertebrates (Ma, 1994a,b). This reduction in noradrenergic innervation could induce a subsequent reduction of presynaptic α_2 adrenergic receptor binding sites in target areas that receive afferents by LoC, such as telencephalic Dm areas and cerebellum.

Further examination of the relative numbers of α_2 and β AR populations during postnatal life indicated their specific roles in development and revealed some interesting distribution patterns. For this, we calculated the ratio of α_2/β AR densities for all measured areas within each
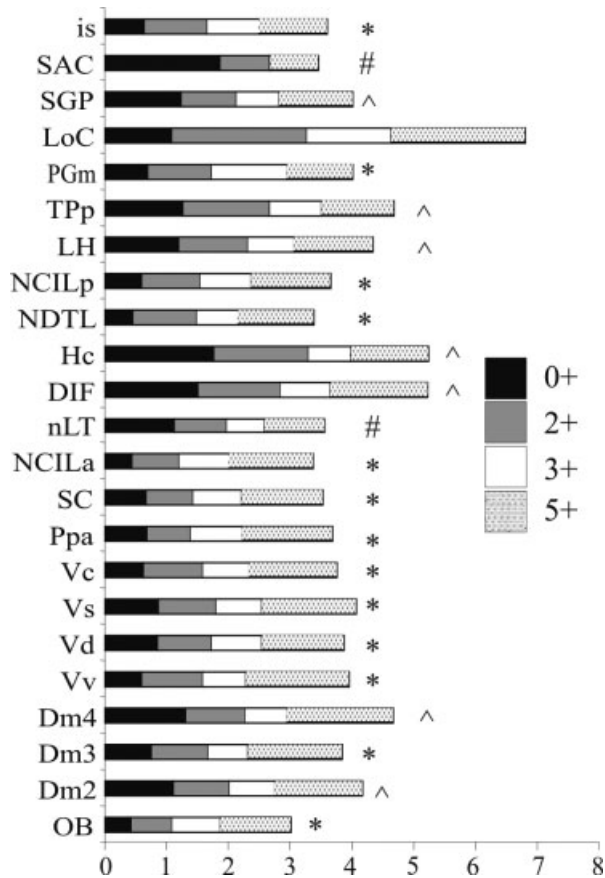
Fig. 11. Differential α_2/β AR density ratio in measured teleost brain areas, throughout development. The symbols indicate AR phenotype predominance change with age as follows: *shift from β to α_2 AR; #shift from α_2 to β AR; ^ transient shift from α_2 to β AR at the age of 2 or 3+ years.

ences in AR type ratio is not yet understood but could be related to a presynaptic role (regulating noradrenaline release) and a postsynaptic function (mediating noradrenaline functions) of α_2 AR as known for adult avian and mammalian brain. In addition, the rate of growth and proliferative activity declines with age (Ling et al., 1997; Zikopoulos et al., 2000), resulting in the reduction of newborn cells that are suggested to express various adrenergic receptors (Wang and Lidow, 1997). One could assume that such changes in the addition and integration of the newly generated neurons (Zupanc et al., 1996) could be reflected in the density and type of noradrenergic receptors in specific brain regions. Moreover, these time-course alterations in receptor type densities could be related to their differential localization in neuronal cells, as was shown in the immunocytochemical experiments. Their specific dendritic, perikaryal, or axonal distribution could be associated with the maturation course of specific cellular elements.

Furthermore, the additional expression of α_{2A}, β_1, and β_2 AR by astrocytes could account, at least in part, for the changes in the receptor developmental pattern in areas rich in glia. This is the case for midline nuclei, located adjacent to adult proliferation zones (Zikopoulos et al., 2000), rich in radial glia, which guide newborn cells during their migration (Zupanc and Clint, 2003). Indeed, reorganization of the supporting glial network following changes in the cell proliferation rate with age (Ling et al., 1997; Zikopoulos et al., 2001) could in turn lead to the AR modulation. It is worth noting that the dorsomedial part of CCbmol, which coincides with the dorsal cerebellar proliferation zone in adult fish (Zupanc et al., 1996; Zikopoulos et al., 2000), consistently exhibited the highest density of β AR and moderate to high α_2 AR density. Purkinje cell dendrites are absent or very sparse in this area, and positive immunohistochemical detection with α_{2A}, β_1, and β_2 AR antibodies coexpressed with GFAP clearly indicates the presence of these receptors in radial glia fibers. This specific proliferation zone is by far the most active in the whole teleostean brain, and newborn neurons have been shown to interact with radial glial cells at least during migration along those fiber paths (Zupanc and Clint, 2003; our unpublished observations). Adrenergic receptor-positive glial cells were found in almost all periventricular proliferation zones, which in most cases include moderate to high levels of receptor binding sites, demonstrating a possible important role of the noradrenergic system in developing and adult neurogenesis and cell migration.

Complex events possibly relate to the cerebellar adrenergic receptor development that follows similar pattern among vertebrates. Indeed, α_2 AR postnatal development is conserved among vertebrates (Dermon and Kouvelas, 1988; Flügge et al., 1993; Happe et al., 1999, 2004), in agreement with the present study reporting that earlier developmental stages exhibited higher α_2 AR levels than later and mature stages. This loss of cerebellar α_2 AR could be related to apoptotic neuronal or glial cell death, as suggested for developing mouse cerebellum (Ashwell, 1990; Flügge et al., 1993), although teleostean cerebellum is characterized by enormous proliferative capacity (Zikopoulos et al., 2000; Zupanc and Clint, 2003). Another possibility could be a down-regulation mechanism induced by high local concentrations of agonists (Raymond et al., 1990). Alternatively, changes in receptor densities could be related to changes in noradrenergic afferents, particu-

age group; 0+, 2+, 3+ and 5+ (Fig. 11). As would be expected, the majority of brain areas preserved their receptor ratio during development (Fig. 11). At the earliest age (0+) studied, most cases included higher density of β sites compared with α_2 AR, with the exception of dorsal hypothalamic areas (dHA, nRL), periventricular ventral and caudal hypothalamus (Hv, Hc), and diffuse nucleus of inferior lobe (DIF), that preserved this α_2 AR predominance in adult life. Few regions were characterized by a clear predominance of the β AR type, preserved during all developmental stages studied, such as glomerular nucleus (G) and semicircular torus (TS4) and cerebellar molecular layer, medial granular eminence, and longitudinal torus (CCbmol, Egm, tlo, respectively). However, in some brain areas, the initial β AR predominance ($\alpha_2/\beta < 1$) at 0+, or initial equal ratio of β vs. α_2 AR, was modified at 5+, leading to final α_2 AR prevalence ($\alpha_2/\beta > 1$), as is the case for dorsal (Dm3, Dm4) and ventral (OB, Vv, Vd, Vs, Vc) telencephalic areas, preoptic (PPa, SC), lateral hypothalamic (NCILa, NCILp, NDTL), preglomerular (PGm), LoC, and isthmic (is) nuclei. For example, LoC, at 0+ stage, included a 1/1 ratio of α_2/β AR, whereas, from 2+ stage to adulthood, it included twofold higher α_2 AR vs. β AR density. The functional significance of these differ-

larly in the case of a presynaptic α_2 AR population, as suggested by the immunocytochemical localization of α_2 AR on Purkinje cell somata.

Although there are no reports on the postembryonic development of teleostean noradrenergic innervation, there are several studies describing age-dependent changes in the serotonergic system of various teleosts (for review see Ekström, 1994). The reported plasticity is usually linked to significant physiological events, such as the parr–smolt transformation in salmonids and reproductive state and fecundity in cyprinids, and is expressed through transient changes in neurotransmitter phenotype, increases in neurite branching or neuronal numbers, and changes in serotonin turnover or enzyme activity during aging. The observed noradrenergic system plasticity could also be partially linked to the state of maturity and/or fecundity of the animals used, as has been reported in the case of β_1 and β_2 AR level alterations in female rats (Weiland and Wise, 1986). This is supported by the fact that major hormonal changes occur at about the age of 2 and 3+ years, when testosterone, 17β-estradiol, and vitellogenin levels begin their gradual increase toward adult levels, which are reached between ages 3+ and 5+ years (Kokokiris et al., 1999). The late significant increases of α_2 AR density at 5+ stage found in ventral telencephalic area and periventricular ventral and caudal hypothalamus following initial decreases of α_2 AR during the stages studied could be related to physiological adaptations in hormonal levels. In addition, other factors, such as stress (Flügge et al., 2003), environmental enrichment (Woo and Leon, 1995), experiences (Stamatakis et al., 1998), and social status (Flügge et al., 1992; Dubini et al., 1997), could also participate in the determination of noradrenergic innervation and receptor levels.

Anatomical and functional correlations of adrenergic receptors: comparison with other vertebrates

The comparison of receptor density and distribution among species has been a useful tool for the study of the phylogeny of various brain areas (Dietl and Palacios, 1988). Few existing studies on the distribution of noradrenergic immunoreactivity in amphibian brain are in general agreement with equivalent studies in teleosts (Gonzalez and Smeets, 1993, 1995; for review see Smeets and Gonzalez, 2000), allowing us to infer some correlations, wherever applicable. In addition, the conservation of the adrenergic receptor properties allowed comparisons with birds and mammals, even though, teleosts diverted early in phylogeny. One has to keep in mind though that several teleostean brain structures might have evolved independently of the respective tetrapod areas and thus may be examples of homoplasy.

Telencephalon. Dorsal telencephalon consists mainly of dorsomedial, dorsolateral, dorsal, lateral, and posterior sectors. Higher α_2 AR binding sites were found in the dorsomedial zone, thought to be a limbic-like area, homologous to the pallial amygdala (Braford, 1995; Portavella et al., 2002). Autoradiographic binding studies in mammals (Unnerstall et al., 1984; Pazos et al., 1988) and birds (Fernandez-Lopez et al., 1997) have also shown higher α_2 AR in this region, in accordance with the present study. Moreover, in situ hybridization and immunohistochemical studies indicate the predominance of the α_{2A} subtype,

among α_2 AR (Nicholas et al., 1993a; Talley et al., 1996), in agreement with our findings. The adjacent dorsolateral zone (DL) is involved in spatial-temporal learning and memory processes in teleosts, resembling hippocampal functions of other vertebrates (Portavella et al., 2002; Rodriguez et al., 2002), and included moderate AR levels, comparable to those of the caudoventral region of mammalian hippocampus (Unnerstall et al., 1984). The present evidence on AR autoradiographic densities and immunohistochemistry further supports the hypothesis that teleostean DL resembles the caudoventral part of mammalian hippocampus (Portavella et al., 2002). This notion is strengthened by the β_2 AR predominance, which has also been reported for mammals (Nicholas et al., 1993b). This is not the case for the avian hippocampal area, which exhibits low levels of α_2 and moderate levels of β AR binding (Ball et al., 1989; Fernandez-Lopez et al., 1997), although homology is not well established. More dorsally located telencephalic areas (Dd, Dld) are considered homologous to the dorsal pallium/isocortex of amniotes (Braford, 1995; Butler and Hodos, 1996; Butler, 2000). This is in agreement with the receptor profile of these teleostean areas, in that moderate to high levels of α_2 and β AR binding have also been reported in avian (Dermon and Kouvelas, 1989; Fernandez-Lopez et al., 1997) and mammalian (Palacios and Kuhar, 1980; Pazos et al., 1988) brains.

The ventral telencephalic area is suggested to be subpallial in teleosts, with the dorsal zone (Vd, Vc, Vs) representing the striatum, and the ventrolateral (Vv, Vl) the septum (Butler and Hodos, 1996; Wullimann and Rink, 2002). The findings for the latter, with its relatively high α_2 and β AR binding and its preponderant α_{2A} immunoreactivity, correlate well with reports on mammals (Unnerstall et al., 1984; Talley et al., 1996; Smeets and Gonzalez, 2000) and birds (Ball et al., 1989; Fernandez-Lopez et al., 1997). However, the dorsal zone of ventral telencephalon, including dendritic and in small or medium-sized neurons α_{2C} and β_2 immunoreactivity, showed moderate levels of both receptors, in contrast to low levels of α_2 and high β AR binding sites reported in mammals (Palacios and Kuhar, 1980; Unnerstall et al., 1984; Pazos et al., 1988).

Diencephalon. In most teleostean diencephalic areas, the AR profile is comparable to that obtained from studies of avian and mammalian brain. Specifically, the presence of high densities of α_2 AR in the teleostean hypothalamus is in agreement with mammalian (Unnerstall et al., 1984) and avian (Ball et al., 1989; Dermon and Kouvelas, 1989; Fernandez-Lopez et al., 1997) studies. In the present study, an anteroposterior gradient in α_{2A} AR density was evident. Highly immunoreactive α_{2A} and α_{2C} AR fibers were located in the vicinity of medial and lateral periventricular surfaces, whereas β_1 and β_2 AR-ir fibers were uniformly spread. Clusters of small α_{2A} and α_{2C} AR-ir neurons were gathered around the lateral and posterior recesses and along the ventral midline. Medium-sized and large neurons stained for all subtypes were scattered in the inferior lobes, the lateral torus, and toward the midline. Our results combined with those of Aoki et al. (1994) and Talley et al. (1996) indicate that hypothalamic α_{2A} AR immunoreactivity is substantial in vertebrates.

However, there are discrepancies in AR distribution between the teleostean posterior tuberculum (TP) and caudal hypothalamus (Hc) and their suggested compara-

ble areas in amniotes, the substancia nigra/ventral tegmental area (SN/VTA; Kaslin and Panula, 2001; Rink and Wullimann, 2001). Specifically, although β AR binding levels were found to be comparable, the pattern of α_2 AR binding was not in agreement with that of the mammalian or avian SN/VTA, which exhibits low AR levels (for SN/VTA; Unnerstall et al., 1984; Dermon and Kouvelas, 1989; Fernandez-Lopez et al., 1997). Moreover, whereas α_{2A} AR-ir elements are prominent in teleostean TP/Hc, α_{2C} AR immunoreactivity prevails in mammalian SN/VTA.

Mesencephalon. Sensory integration centers, the optic tectum (mostly visual input; superior colliculus in mammals; Butler and Hodos, 1996) and the semicircular torus (mostly acoustic and lateral line input; inferior colliculus in mammals; Butler and Hodos, 1996), contained moderate levels of α_2 and β AR binding sites in a layer-specific pattern, in accordance with the layer topography of immunocytochemical labeling; that is, superficial tectal layers contained significantly higher numbers of medium-sized α_{2A}, β_1 and β_2 AR-ir neurons and fibers than deeper periventricular layer (SGP), which included small neurons positive for α_{2A}, β_1, and β_2 AR. This is similar to the pattern described for birds (Ball et al., 1989; Dermon and Kouvelas, 1989; Fernandez-Lopez et al., 1997) and mammals (Palacios and Kuhar, 1980; Unnerstall et al., 1984), highlighting a similar role of the noradrenergic system in sensory modulation and integration among vertebrates. In addition, the preserved topography and layer-specific pattern of adrenergic receptors possibly reflect the evolutionary preservation of the local cytoarchitecture and circuits of these areas. Moreover, it should be noted that the visual sensory circuit from superficial tectal layers, their target thalamic regions (mainly preglomerular; Ito et al., 1980a,b; Ito and Vanegas, 1984; Murakami et al., 1986; Peyrichoux et al., 1986), and the dorsal telencephalic areas that are in turn reciprocally connected with the thalamic areas (Echteler and Saidel, 1981; Murakami et al., 1983, 1986) all included high or moderate α_2 and β AR binding levels, indicating the important role of AR in visual sensory information integration.

Tegmentum. Autoradiographic studies with a variety of α_2 AR agonists and antagonists in most vertebrates parallel our results, demonstrating that the most prominently labeled region in the dorsal pons is the LoC (Unnerstall et al., 1984; Dermon and Kouvelas, 1989). There is general agreement about the expression of α_{2A} AR subtypes in LoC (Nicholas et al., 1993a; Lee et al., 1998a), but the existence of other receptor subtypes is less well documented (Nicholas et al., 1996; Rosin et al., 1996; Lee et al., 1998b). The surrounding mammalian isthmal area and midbrain tegmentum, including the motor nuclei, the raphe complex, and the reticular formation, are rich in both α_2 and β AR binding sites and express substantial α_{2A}, α_{2C}, β_1, and β_2 immunoreactivity (Palacios and Kuhar, 1980; Unnerstall et al., 1984; Wanaka et al., 1989; Nicholas et al., 1993a,b; Smeets and Gonzalez, 2000), well correlated with the observed pattern in the teleostean comparable areas.

Cerebellum. The α_2 and β AR distributions in the cerebellum were consistent with the distribution of those receptors in avian (Dermon and Kouvelas, 1989; Fernandez-Lopez et al., 1997) and mammalian (Palacios and Kuhar, 1980; Unnerstall et al., 1984) cerebellum, for which negligible α_2 and high β AR densities, especially in the molecular and Purkinje cell layers, have been reported. In addition, the vast majority of adrenergic binding sites were found to be of β_2 subtype, as in avian (Dermon and Kouvelas 1988) and mammalian (Palacios and Kuhar 1980) cerebellum.

Taken together, our data on α_2 and β AR properties, glial and neuronal localization, further support the AR conservation among vertebrates, even in evolutionarily distant species. The addition of data on regional specificity and developmental pattern of α_2 and β AR not only presents valuable information on the development of vertebrate CNS but also highlights the conserved vs. the diverse character of vertebrate brain evolution.

LITERATURE CITED

Aoki C, Go CG, Venkatesan C, Kurose H. 1994. Perikaryal and synaptic localization of alpha 2A-adrenergic receptor-like immunoreactivity. Brain Res 650:181–204.

Ashwell K. 1990. Microglia and cell death in the developing mouse cerebellum. Brain Res Dev Brain Res 55:219–230.

Ball GF, Nock B, McEwen BS, Balthazart J. 1989. Distribution of alpha 2-adrenergic receptors in the brain of the Japanese quail as determined by quantitative autoradiography: implications for the control of sexually dimorphic reproductive processes. Brain Res 491:68–79.

Berridge CW, Waterhouse BD. 2003. The locus coeruleus-noradrenergic system: modulation of behavioural state and state-dependent cognitive processes. Brain Res Rev 42:32–84.

Braford MR. 1995. Comparative aspects of forebrain organization in the ray-finned fishes: touchstones or not? Brain Behav Evol 46:259–274.

Braford MRJ, Northcutt RG. 1983. Organization of the diencephalon and pretectum of the ray-finned fishes. In: Northcutt RG, Davis RE, editors. Fish neurobiology. Ann Arbor: The University of Michigan Press. p 88–140.

Brantley RK, Bass AH. 1988. Cholinergic neurons in the brain of a teleost fish (*Porichthys notatus*) located with a monoclonal antibody to choline acetyltransferase. J Comp Neurol 275:87–105.

Butler AB. 2000. Topography and topology of the teleost telencephalon: a paradox resolved. Neurosci Lett 293:95–98.

Butler AB, Hodos W. 1996. Comparative vertebrate neuroanatomy. Evolution and adaptation. New York: Wiley-Liss.

Bylund DB. 1992. Subtypes of alpha 1- and alpha 2-adrenergic receptors. FASEB J 6:832–839.

Bylund DB, Eikenberg DC, Hieble JP, Langer SZ, Lefkowitz RJ, Minneman KP, Molinoff PB, Ruffolo RR, Trendelenburg U. 1994. International Union of Pharmacology nomenclature of adrenoceptors. Pharmacol Rev 46:121–136.

Charney DS. 1998. Monoamine dysfunction and the pathophysiology and treatment of depression. J Clin Psychiatry 59(Suppl 14):11–14.

Civantos-Calzada B, Aleixandre-de-Artiñano A. 2001. Alpha-adrenoceptor subtypes. Pharmacol Res 44:195–208.

Cooney MM, Conaway CH, Mefford IN. 1985. Epinephrine, norepinephrine, and dopamine concentrations in amphibian brain. Comp Biochem Physiol 82C:395–397.

DeVos H, Vauquelin G, De Keyser J, De Backer JP, Van Liefde I. 1992. Regional distribution of alpha 2A- and alpha 2B-adrenoceptor subtypes in postmortem human brain. J Neurochem 58:1555–1560.

Dermon CR, Kouvelas ED. 1988. Binding properties, regional ontogeny and localization of adrenergic receptors in chick brain. Int J Dev Neurosci 6:471–482.

Dermon CR, Kouvelas ED. 1989. Quantitative analysis of the localization of adrenergic binding sites in chick brain. J Neurosci Res 23:297–303.

Dietl M, Palacios JM. 1988. Receptor autoradiography as a tool for the study of the phylogeny of the basal ganglia. J Recept Res 8:521–532.

Divanach P, Kentouri M, Charalambakis G, Pouget F, Sterioti A. 1993. Comparison of growth performance of six Mediterranean species reared under intensive farming conditions in Crete (Greece), in raceways with the use of self feeders. In: Barnabe G, Kestemont P, editors. Production, environment and quality. Bordeaux Aquaculture '92. Special Publication No. 18. Ghent: European Aquaculture Society. p 285–297.

Dubini A, Bosc M, Polin V. 1997. Do noradrenaline and serotonin differentially affect social motivation and behaviour? Eur Neuropsychopharmacol 7(Suppl 1):S49–S55 [discussion S71–S73].

Dygalo NN, Kalinina TS, Sournina NY, Shishkina GT. 2002. Effects of testosterone on alpha2A-adrenergic receptor expression in the rat brain. Psychoneuroendocrinology 27:585–592.

Echteler SM, Saidel WM. 1981. Forebrain connections in the goldfish support telencephalic homologies with land vertebrates. Science 212:683–685.

Ekstrom P. 1994. Developmental changes in the brain-stem serotonergic nuclei of teleost fish and neural plasticity. Cell Mol Neurobiol 14:381–393.

Ekstrom P, Reschke M, Steinbusch H, van Veen T. 1986. Distribution of noradrenaline in the brain of the teleost Gasterosteus aculeatus L.: an immunohistochemical analysis. J Comp Neurol 254:297–313.

Erdtsieck-Ernste EB, Feenstra MG, Boer GJ, van-Galen H. 1991. Chronic propranolol treatment in developing rats: acute and lasting effects on monoamines and beta-adrenergic receptors in the rat brain. Brain Res Bull 26:731–737.

Etgen AM, Karkanias GB. 1994. Estrogen regulation of noradrenergic signaling in the hypothalamus. Psychoneuroendocrinology 19:603–610.

Fernandez-Lopez A, Revilla V, Candelas MA, Gonzalez-Gil J, Diaz A, Pazos A. 1997. A comparative study of alpha2- and beta-adrenoceptor distribution in pigeon and chick brain. Eur J Neurosci 9:871–883.

Finkenbine SS, Gettys TW, Burnett KG. 2002. Beta-adrenergic receptors on leukocytes of the channel catfish, Ictalurus punctatus. Comp Biochem Physiol C131:27–37.

Flügge G, Johren O, Fuchs E. 1992. [^{3}H]rauwolscine binding sites in the brains of male tree shrews are related to social status. Brain Res 597:131–137.

Flügge G, Brandt S, Fuchs E. 1993. Postnatal development of central nervous system alpha 2-adrenergic binding sites: an in vitro autoradiography study in the tree shrew. Brain Res Dev Brain Res 74:163–175.

Flügge G, van Kampen M, Meyer H, Fuchs E. 2003. Alpha2A and alpha2C-adrenoceptor regulation in the brain: alpha2A changes persist after chronic stress. Eur J Neurosci 17:917–928.

Forlano PM, Deitcher DL, Myers DA, Bass AH. 2001. Anatomical distribution and cellular basis for high levels of aromatase activity in the brain of teleost fish: aromatase enzyme and mRNA expression identify glia as source. J Neurosci 21:8943–8955.

Gonzalez A, Smeets WJAJ. 1993. Noradrenaline in the brain of the South African clawed frog Xenopus laevis: a study with antibodies against noradrenaline and dopamine-beta-hydroxylase. J Comp Neurol 331:363–374.

Gonzalez A, Smeets WJAJ. 1995. Noradrenergic and adrenergic systems in the brain of the urodele amphibian, Pleurodeles waltlii, as revealed by immunohistochemical methods. Cell Tissue Res 279:619–627.

Goodman RL, Havern RL, Whisnant CS. 1996. Alpha adrenergic neurons inhibit luteinizing hormone pulse amplitude in breeding season ewes. Biol Reprod 54:380–386.

Granneman JG, Lahners KN, Chaudhry A. 1991. Molecular cloning and expression of the rat beta 3-adrenergic receptor. Mol Pharmacol 40:895–899.

Hamilton CA, Howe CA, Reid JL. 1984. Changes in brain alpha-adrenoceptors with increasing age in rabbits. Brain Res 322:177–179.

Happe HK, Bylund DB, Murrin LC. 1999. Alpha-2 adrenergic receptor functional coupling to G proteins in rat brain during postnatal development. J Pharmacol Exp Ther 288:1134–1142.

Happe HK, Coulter CL, Gerety ME, Sanders JD, O'Rourke M, Byland DB, Murrin LC. 2004. Alpha-2 adrenergic receptor development in rat CNS: An autoradiographic study. Neuroscience 123:167–178.

Harris PJ, McGovern JC. 1997. Changes in the life history of red porgy, Pagrus pagrus, from the southeastern United States, 1972–1994. Fish Bull 95:742–747.

Harro J, Oreland L. 2001. Depression as a spreading adjustment disorder of monoaminergic neurons: a case for primary implication of the locus coeruleus. Brain Res Brain Res Rev 38:79–128.

Herman CA, Luczy SE, Wikberg JES, Uhlen S. 1996. Characterization of adrenoceptor types and subtypes in American bullfrogs acclimated to warm or cold temperature. Gen Comp Endocrinol 104:168–178.

Hodges-Savola C, Rogers SD, Ghilardi JR, Timm DR, Mantyh PW. 1996. Beta-adrenergic receptors regulate astrogliosis and cell proliferation in the central nervous system in vivo. Glia 17:52–62.

Holmgren S, Nilsson S. 1982. Neuropharmacology of adrenergic neurons in teleost fish. Comp Biochem Physiol C72:289–302.

Ito H, Vanegas H. 1984. Visual receptive thalamopetal neurons in the optic tectum of teleosts (Holocentridae). Brain Res 290:201–210.

Ito H, Butler AB, Ebbesson SO. 1980a. An ultrastructural study of the normal synaptic organization of the optic tectum and the degenerating tectal afferents from retina, telencephalon, and contralateral tectum in a teleost, Holocentrus rufus. J Comp Neurol 191:639–659.

Ito H, Morita Y, Sakamoto N, Ueda S. 1980b. Possibility of telencephalic visual projection in teleosts, Holocentridae. Brain Res 197:219–222.

Johnson AE, Nock B, Ryer H, Feder H. 1984. Hypothalamic and preoptic area alpha 1-receptor concentrations decrease, and cerebral cortical alpha 1-receptor concentrations increase during postnatal maturation of male guinea pigs. Neuroendocrinology 38:243–247.

Johnson AE, Nock B, McEwen BS, Feder HH. 1988. Alpha 1- and alpha 2-noradrenergic receptors in steroid-sensitive brain areas: development and response to estradiol-17 beta benzoate in neonatal guinea pigs. Brain Res 470:247–252.

Jones LS, Gauger LL, Davis JN, Slotkin TA, Bartolome JV. 1985. Postnatal development of brain alpha 1-adrenergic receptors: in vitro autoradiography with [^{125}I]HEAT in normal rats and rats treated with alpha-difluoromethylornithine, a specific, irreversible inhibitor of ornithine decarboxylase. Neuroscience 15:1195–1202.

Kalman M. 1998. Astroglial architecture of the carp (Cyprinus carpio) brain as revealed by immunohistochemical staining against glial fibrillary acidic protein (GFAP). Anat Embryol 198:409–433.

Karlsson JO, Andersson RG, Grundstrom N. 1989. Characterization of pigment aggregating alpha 2-adrenoceptors of fish melanophores by use of different agonists after partial irreversible receptor inactivation. Br J Pharmacol 97:222–228.

Kaslin J, Panula P. 2001. Comparative anatomy of the histaminergic and other aminergic systems in zebrafish (Danio rerio). J Comp Neurol 440:342–377.

Katayama H, Morishita F, Matsushima O, Fujimoto M. 1999. Beta-adrenergic receptor subtypes in melanophores of the marine gobies Tridentiger trigonocephalus and Chasmichthys gulosus. Pigment Cell Res 12:206–217.

Kentouri M, Neill OD, Divanach P, Charalambakis G. 1994. A study on the quantitative water requirements of red porgies, Pagrus pagrus, L (Pisces: Sparidae), during early on-growing under self feeding conditions. Aquacult Fish Manag 25:741–752.

Kobilka B. 1992. Adrenergic receptors as models for G protein-coupled receptors. Annu Rev Neurosci 15:87–114.

Kokokiris L, Brusle S, Kentouri M, Fostier A. 1999. Sexual maturity and hermaphroditism of the red porgy Pagrus pagrus (Teleostei: Sparidae). Mar Biol 134:621–629.

Koster G. 1995. Glial alpha 2-receptors probably inhibit the high-affinity uptake of noradrenaline into astrocytes in the rat brain in vivo. Neurochem Res 20:291–297.

Kotrschal K, Van Staaden MJ, Huber R. 1998. Fish brains: evolution and environmental relationships. Rev Fish Biol Fisheries 8:373–408.

Lee A, Rosin DL, Van-Bockstaele EJ. 1998a. Alpha2A-adrenergic receptors in the rat nucleus locus coeruleus: subcellular localization in catecholaminergic dendrites, astrocytes, and presynaptic axon terminals. Brain Res 795:157–169.

Lee A, Wissekerke AE, Rosin DL, Lynch KR. 1998b. Localization of alpha2C-adrenergic receptor immunoreactivity in catecholaminergic neurons in the rat central nervous system. Neuroscience 84:1085–1096.

Ling C, Zuo M, Alvarez-Buylla A, Cheng MF. 1997. Neurogenesis in juvenile and adult ring doves. J Comp Neurol 379:300–312.

Lorton D, Bartolome J, Slotkin TA, Davis JN. 1988. Development of brain beta-adrenergic receptors after neonatal 6-hydroxydopamine treatment. Brain Res Bull 21:591–600.

Ma PM. 1994a. Catecholaminergic systems in the zebrafish. I. Number, morphology, and histochemical characteristics of neurons in the locus coeruleus. J Comp Neurol 344:242–255.

Ma PM. 1994b. Catecholaminergic systems in the zebrafish. II. Projection

pathways and pattern of termination of the locus coeruleus. J Comp Neurol 344:256–269.

Ma PM. 1997. Catecholaminergic systems in the zebrafish. III. Organization and projection pattern of medullary dopaminergic and noradrenergic neurons. J Comp Neurol 381:411–427.

Maler L, Sas E, Johnston S, Ellis W. 1991. An atlas of the brain of the electric fish *Apteronotus leptorhynchus.* J Chem Neuroanat 4:1–38.

Manooch CS, Hassler WW. 1978. Synopsis of biological data on the red porgy, *Pagrus pagrus* (Linnaeus). FAO Fish Synop 116:1–19.

Mantyh PW, Rogers SD, Allen CJ, Catton MD, Ghilardi JR, Levin LA, Maggio JE, Vigna SR. 1995. Beta 2-adrenergic receptors are expressed by glia in vivo in the normal and injured central nervous system in the rat, rabbit, and human. J Neurosci 15:152–164.

McDonald JK, Petrovic SL, McCann SM, Parnavelas JG. 1982. The development of beta-adrenergic receptors in the visual cortex of the rat. Neuroscience 7:2649–2655.

Meek J, Joosten HW, Hafmans TG. 1993. Distribution of noradrenaline-immunoreactivity in the brain of the mormyrid teleost *Gnathonemus petersii.* J Comp Neurol 328:145–160.

Milner TA, Lee A, Aicher SA, Rosin DL. 1998. Hippocampal alpha2a-adrenergic receptors are located predominantly presynaptically but are also found postsynaptically and in selective astrocytes. J Comp Neurol 395:310–327.

Mishra N, Hamilton CA, Jones CR, Reid JL. 1985. The effects of sexual maturation on alpha-adrenoceptors in female rabbits. Eur J Pharmacol 112:243–247.

Morishita F, Katayama H, Yamada K. 1985. Subtypes of beta adrenergic receptors mediating pigment dispersion in chromatophores of the medaka, *Oryzias latipes.* Comp Biochem Physiol C81:279–285.

Murakami T, Morita Y, Ito H. 1983. Extrinsic and intrinsic fiber connections of the telencephalon in a teleost, Sebasticus marmoratus. J Comp Neurol 216:115–131.

Murakami T, Fukuoka T, Ito H. 1986. Telencephalic ascending acoustico-lateral system in a teleost (*Sebastiscus marmoratus*), with special reference to the fiber connections of the nucleus preglomerulosus. J Comp Neurol 247:383–397.

Nahorski SR. 1978. Heterogeneity of cerebral β-adrenoceptor binding sites in various vertebrate species. Eur J Pharmacol 51:199–209.

Nicholas AP, Pieribone V, Hokfelt T. 1993a. Distributions of mRNAs for alpha-2 adrenergic receptor subtypes in rat brain: an in situ hybridization study. J Comp Neurol 328:575–594.

Nicholas AP, Pieribone VA, Hokfelt T. 1993b. Cellular localization of messenger RNA for beta-1 and beta-2 adrenergic receptors in rat brain: an in situ hybridization study. Neuroscience 56:1023–1039.

Nicholas AP, Hokfelt T, Pieribone VA. 1996. The distribution and significance of CNS adrenoceptors examined with in situ hybridization. Trends Pharmacol Sci 17:245–255.

Nickerson JG, Dugan SG, Drouin G, Moon TW. 2001. A putative β_2-adrenoceptor from rainbow trout (*Oncorhynchus mykiss*). Molecular characterization and pharmacology. Eur J Biochem 268:6465–6472.

Nieuwenhuys R, Pouwels E. 1983. The brain stem of actinopterygian fishes. In: Northcutt RG, Davis RE, editors. Fish neurobiology. Ann Arbor: The University of Michigan Press. p 25–87.

Northcutt RG, Davis RE. 1983. Telencephalic organization in ray-finned fishes. In: Northcutt RG, Davis RE, editors. Fish neurobiology. Ann Arbor: The University of Michigan Press. p 142–204.

Ohno M, Watanabe S. 1996. Blockade of 5-HT1A receptors compensates loss of hippocampal cholinergic neurotransmission involved in working memory of rats. Brain Res 736:180–188.

Ordway GA, Jaconetta SM, Halaris AE. 1993. Characterization of subtypes of alpha-2 adrenoceptors in the human brain. J Pharmacol Exp Ther 264:967–976.

Pajuelo JG, Lorenzo JM. 1996. Life history of the red porgy *Pagrus pagrus* (Teleostei: Sparidae) off the Canary Islands, central East Atlantic. Fish Res 28:163–177.

Palacios JM, Kuhar MJ. 1980. Beta-adrenergic-receptor localization by light microscopic autoradiography. Science 208:1378–1380.

Palacios JM, O'Dowd BF, Cotecchia S, Hnatowich M, Caron MG, Lefkowitz RJ. 1989. Adrenergic receptor homologies in vertebrate and invertebrate species examined by DNA hybridization. Life Sci 44:2057–2065.

Pascual J, del-Arco C, Gonzalez AM, Diaz A, del-Olmo E, Pazos A. 1991. Regionally specific age-dependent decline in alpha 2-adrenoceptors: an autoradiographic study in human brain. Neurosci Lett 133:279–283.

Pazos A, Probst A, Palacios JM. 1985. Beta-adrenoceptor subtypes in the human brain: autoradiographic localization. Brain Res 358:324–328.

Pazos A, Gonzalez AM, Pascual J, Meana JJ, Barturen F, Garcia-Sevilla JA. 1988. Alpha 2-adrenoceptors in human forebrain: autoradiographic visualization and biochemical parameters using the agonist [³H]UK-14304. Brain Res 475:361–365.

Peyrichoux J, Pierre J, Reperant J, Rio JP. 1986. Fine structure of the optic fiber termination layer in the tectum of the teleost rutilus: a stereological and morphometric study. J Comp Neurol 246:364–381.

Piantanelli L, Gentile S, Fattoretti P, Viticchi C. 1985. Thymic regulation of brain cortex beta-adrenoceptors during development and aging. Arch Gerontol Geriatr 4:179–185.

Pittman RN, Minneman KP, Molinoff PB. 1980. Ontogeny of beta 1- and beta 2-adrenergic receptors in rat cerebellum and cerebral cortex. Brain Res 188:357–368.

Portavella M, Vargas JP, Torres B, Salas C. 2002. The effects of telencephalic pallial lesions on spatial, temporal, and emotional learning in goldfish. Brain Res Bull 57:397–399.

Potter WZ, Manji HK. 1994. Catecholamines in depression: an update. Clin Chem 40:279–287.

Raymond JR, Hnatowich M, Lefkowitz RJ, Caron MG. 1990. Adrenergic receptors. Models for regulation of signal transduction processes. Hypertension 15:119–131.

Revilla R, Fernandez-Lopez C, Revilla V, Fernandez-Lopez A. 1998. Pre- and post-hatching developmental changes in beta-adrenoceptor subtypes in chick brain. Brain Res Dev Brain Res 111:169–167.

Rink E, Wullimann MF. 2001. The teleostean (zebrafish) dopaminergic system ascending to the subpallium (striatum) is located in the basal diencephalon (posterior tuberculum). Brain Res 889:316–330.

Riters LV, Eens M, Pinxten R, Ball GF. 2002. Seasonal changes in the densities of alpha (2) noradrenergic receptors are inversely related to changes in testosterone and the volumes of song control nuclei in male European starlings. J Comp Neurol 444:63–74.

Rodriguez F, Lopez JC, Vargas JP, Broglio C, Gomez Y, Salas C. 2002. Spatial memory and hippocampal pallium through vertebrate evolution: insights from reptiles and teleost fish. Brain Res Bull 57:499–503.

Rosin DL, Talley EM, Lee A, Stornetta RL, Gaylinn BD, Guyenet PG, Lynch KR. 1996. Distribution of alpha 2C-adrenergic receptor-like immunoreactivity in the rat central nervous system. J Comp Neurol 372:135–165.

Ruuskanen JO, Xhaard H, Marjamaki A, Salaneck E, Salminen T, Yan Y-L, Postlethwait JH, Johnson MS, Larhammar D, Scheinin M. 2004. Identification of duplicated fourth α_2-adrenergic receptor subtype by cloning and mapping of five receptor genes in zebrafish. Mol Biol Evol 21:14–28.

Sas E, Maler L, Tinner B. 1990. Catecholaminergic systems in the brain of a gymnotiform teleost fish: an immunohistochemical study. J Comp Neurol 292:127–162.

Sastre M, Guimon J, Garcia-Sevilla JA. 2001. Relationships between beta- and alpha2-adrenoceptors and G coupling proteins in the human brain: effects of age and suicide. Brain Res 898:242–255.

Shishkina GT, Kalinina TS, Sournina NY, Dygalo NN. 2001. Effects of antisense to the (alpha)2A-adrenoceptors administered into the region of the locus ceruleus on behaviors in plus-maze and sexual behavior tests in sham-operated and castrated male rats. J Neurosci 21:726–731.

Smeets WJ, Gonzalez A. 2000. Catecholamine systems in the brain of vertebrates: new perspectives through a comparative approach. Brain Res Brain Res Rev 33:308–379.

Stamatakis A, Stewart MG, Dermon CR. 1998. Passive avoidance learning involves α_2-noradrenergic receptors in a day old chick. Neuroreport 9:1679–1683.

Svensson SP, Bailey TJ, Pepperl DJ, Grundstrom N, Ala-Uotila S, Scheinin M, Karlsson JO, Regan JW. 1993. Cloning and expression of a fish alpha 2-adrenoceptor. Br J Pharmacol 110:54–60.

Talley EM, Rosin DL, Lee A, Guyenet PG, Lynch KR. 1996. Distribution of alpha 2A-adrenergic receptor-like immunoreactivity in the rat central nervous system. J Comp Neurol 372:111–134.

Toyoda J, Uematsu K. 1994. Brain morphogenesis of the red sea bream, *Pagrus major* (teleostei). Brain Behav Evol 44:324–37.

Uhlen S, Lindblom J, Johnson A, Wikberg JE. 1997. Autoradiographic studies of central alpha 2A- and alpha 2C-adrenoceptors in the rat using [³H]MK912 and subtype-selective drugs. Brain Res 770:261–266.

Unnerstall JR, Kopajtic TA, Kuhar MJ. 1984. Distribution of alpha 2 agonist binding sites in the rat and human central nervous system:

analysis of some functional, anatomic correlates of the pharmacologic effects of clonidine and related adrenergic agents. Brain Res 319:69–101.

Unnerstall JR, Fernandez I, Orensanz LM. 1985. The alpha-adrenergic receptor: radiohistochemical analysis of functional characteristics and biochemical differences. Pharmacol Biochem Behav 22:859–874.

Vassilopoulou V, Papaconstantinou C. 1992. Age, growth and mortality of the red porgy, *Pagrus pagrus*, in the eastern Mediterranean Sea (Dodecanese, Greece). Vie Milieu 42:51–55.

Wanaka A, Kiyama H, Murakami T, Matsumoto M, Kamada T, Malbon CC, Tohyama M. 1989. Immunocytochemical localization of beta-adrenergic receptors in the rat brain. Brain Res 485:125–140.

Wang F, Lidow MS. 1997. Alpha 2A-adrenergic receptors are expressed by diverse cell types in the fetal primate cerebral wall. J Comp Neurol 378:493–507.

Weiland NG, Wise PM. 1986. Effects of age on beta 1- and beta 2-adrenergic receptors in the brain assessed by quantitative autoradiography. Brain Res 398:305–312.

Winzer-Serhan UH, Leslie FM. 1999. Expression of alpha2A adrenoceptors during rat neocortical development. J Neurobiol 38:259–269.

Winzer-Serhan UH, Raymon HK, Broide RS, Chen Y, Leslie FM. 1997a. Expression of alpha 2 adrenoceptors during rat brain development—I. Alpha 2A messenger RNA expression. Neuroscience 76:241–260.

Winzer-Serhan UH, Raymon HK, Broide RS, Chen Y, Leslie FM. 1997b. Expression of alpha 2 adrenoceptors during rat brain development—II. Alpha 2C messenger RNA expression and [^{3}H]rauwolscine binding. Neuroscience 76:261–272.

Woo CC, Leon M. 1995. Distribution and development of beta-adrenergic receptors in the rat olfactory bulb. J Comp Neurol 352:1–10.

Wullimann MF, Rink E. 2002. The teleostean forebrain: a comparative and developmental view based on early proliferation, Pax6 activity and catecholaminergic organization. Brain Res Bull 57:363–370.

Wullimann MF, Rupp B, Reichert H. 1996. Neuroanatomy of the zebrafish brain: a topological atlas. Basel: Birkhäuser.

Zikopoulos B, Kentouri M, Dermon CR. 2000. Proliferation zones in the adult brain of a sequential hermaphrodite teleost species (*Sparus aurata*). Brain Behav Evol 56:310–322.

Zikopoulos B, Kentouri M, Dermon CR. 2001. Cell genesis in the hypothalamus is associated to the sexual phase of a hermaphrodite teleost. Neuroreport 12:2477–2481.

Zupanc GK, Clint SC. 2003. Potential role of radial glia in adult neurogenesis of teleost fish. Glia 43:77–86.

Zupanc GK, Horschke I. 1995. Proliferation zones in the brain of adult gymnotiform fish: a quantitative mapping study. J Comp Neurol 353:213–233.

Zupanc GKH, Horschke I, Ott R, Rascher GB. 1996. Postembryonic development of the cerebellum in gymnotiform fish. J Comp Neurol 370:443–464.